Cellular/Molecular

Promoted Interaction of C/EBPα with Demethylated *Cxcr3* Gene Promoter Contributes to Neuropathic Pain in Mice

Bao-Chun Jiang,[1] Li-Na He,[1] Xiao-Bo Wu,[1] Hui Shi,[1] Wen-Wen Zhang,[1] Zhi-Jun Zhang,[1] De-Li Cao,[1] Chun-Hua Li,[1] Jun Gu,[1] and Yong-Jing Gao[1,2]

[1]Pain Research Laboratory, Institute of Nautical Medicine, Jiangsu Key Laboratory of Inflammation and Molecular Drug Target, and [2]Co-Innovation Center of Neuroregeneration, Nantong University, Jiangsu 226001, China

DNA methylation has been implicated in the pathogenesis of chronic pain. However, the specific genes regulated by DNA methylation under neuropathic pain condition remain largely unknown. Here we investigated how chemokine receptor CXCR3 is regulated by DNA methylation and how it contributes to neuropathic pain induced by spinal nerve ligation (SNL) in mice. SNL increased *Cxcr3* mRNA and protein expression in the neurons of the spinal cord. Meanwhile, the CpG (5′-cytosine-phosphate-guanine-3′) island in the *Cxcr3* gene promoter region was demethylated, and the expression of DNA methyltransferase 3b (DNMT3b) was decreased. SNL also increased the binding of CCAAT (cytidine– cytidine–adenosine–adenosine–thymidine)/enhancer binding protein α (C/EBPα) with *Cxcr3* promoter and decreased the binding of DNMT3b with *Cxcr3* promoter in the spinal cord. C/EBPα expression was increased in spinal neurons after SNL, and inhibition of C/EBPα by intrathecal small interfering RNA attenuated SNL-induced pain hypersensitivity and reduced *Cxcr3* expression. Furthermore, SNL-induced mechanical allodynia and heat hyperalgesia were markedly reduced in *Cxcr3*$^{-/-}$ mice. Spinal inhibition of *Cxcr3* by shRNA or CXCR3 antagonist also attenuated established neuropathic pain. Moreover, CXCL10, the ligand of CXCR3, was increased in spinal neurons and astrocytes after SNL. Superfusing spinal cord slices with CXCL10 enhanced spontaneous EPSCs and potentiated NMDA-induced and AMPA-induced currents of lamina II neurons. Finally, intrathecal injection of CXCL10 induced CXCR3-dependent pain hypersensitivity in naive mice. Collectively, our results demonstrated that CXCR3, increased by DNA demethylation and the enhanced interaction with C/EBPα, can be activated by CXCL10 to facilitate excitatory synaptic transmission and contribute to the maintenance of neuropathic pain.

Key words: astrocyte; CEBPα; CXCL10; CXCR3; demethylation; neuropathic pain

Significance Statement

Peripheral nerve injury induces changes of gene expression in the spinal cord that may contribute to the pathogenesis of neuropathic pain. CXCR3 is a chemokine receptor. Whether it is involved in neuropathic pain and how it is regulated after nerve injury remain largely unknown. Our study demonstrates that spinal nerve ligation downregulates the expression of DNMT3b, which may cause demethylation of *Cxcr3* gene promoter and facilitate the binding of CCAAT/enhancer binding protein α with *Cxcr3* promoter and further increase CXCR3 expression in spinal neurons. The upregulated CXCR3 may contribute to neuropathic pain by facilitating central sensitization. Our study reveals an epigenetic mechanism underlying CXCR3 expression and also suggests that targeting the expression or activation of CXCR3 signaling may offer new therapeutics for neuropathic pain.

Introduction

Neuropathic pain resulting from nerve injury or disease is a highly debilitating chronic pain state and is often resistant to currently available treatments (Toth et al., 2009). Nerve injury induces changes in gene expression in sensory neurons of the dorsal root ganglion and spinal cord. Such changes are thought to influence the pathogenesis of neuropathic pain (Lacroix-Fralish et al., 2006; von Hehn et al., 2012; Jiang et al., 2016). Revealing the molecular mechanisms underlying the dysregulated gene expres-

Received July 16, 2016; revised Nov. 22, 2016; accepted Dec. 2, 2016.

Author contributions: Y.-J.G. designed research; B.-C.J., L.-N.H., X.-B.W., H.S., W.-W.Z., Z.-J.Z., D.-L.C., C.-H.L., and J.G. performed research; B.-C.J., L.-N.H., X.-B.W., W.-W.Z., and Y.-J.G. analyzed data; B.-C.J., X.-B.W., and Y.-J.G. wrote the paper.

This work was supported by grants from the National Natural Science Foundation of China (NSFC 31371121, 81300954, 81400915, and 31671091), the National Science Foundation for Young Scientists of Jiangsu Province (BK20140427), the Natural Science Research Program of Jiangsu Province (13KJB180017), the Innovation Fund for Graduate Students in Nantong University (YKC16021), and the Priority Academic Program Development of Jiangsu Higher Education Institutions. We thank Prof. Gary R. Strichartz for critical reading and language editing of the manuscript. We also thank Prof. Ru-Rong Ji for providing somatostatin (Sst)-Tomato $^{+}$ and Gad2-Tomato $^{+}$ mice.

The authors declare no competing financial interests.

B.-C.J., L.-N.H., X.-B.W., and H.S. contributed equally to this work.

sion under neuropathic pain condition is important for the discovery of new treatments.

Epigenetic regulations, including DNA methylation, histone modification, and noncoding RNA expression, play important roles in the modulation of gene expression. Functionally, these processes are involved in many physiological and pathological processes, including learning and memory (Bali et al., 2011; Zovkic et al., 2013), addiction (Tuesta and Zhang, 2014), cancer (Suzuki et al., 2012; Ma et al., 2013), neurodegenerative disease (Sanchez-Mut and Gräff, 2015), and chronic pain (Descalzi et al., 2015; Liang et al., 2015). DNA methylation is a key epigenetic mechanism controlling DNA accessibility and gene expression (Jaenisch and Bird, 2003). Evidence has shown that nerve injury changes the spinal global DNA methylation (Wang et al., 2011) and that blockade of DNA methylation affects pain behaviors implicated in chronic pain (Wang et al., 2011; Viet et al., 2014). However, the specific genes regulated by DNA methylation and its implication in neuropathic pain remain to be investigated.

Neuroinflammation, mediated by proinflammatory cytokines and chemokines, may play a pivotal role in the development and maintenance of neuropathic pain (White and Wilson, 2008; Abbadie et al., 2009; Gao and Ji, 2010). Several chemokines, such as CXCL13, CCL2, CXCL1, and CX3CL1, are upregulated in the spinal cord after nerve injury or tissue inflammation (Lindia et al., 2005; Gao et al., 2009; Zhang et al., 2013; Jiang et al., 2016). Using mouse gene-expression microarrays, we recently found that the gene for chemokine, *Cxcl10*, is one of the highly upregulated genes with >5-fold increase in the spinal cord after spinal nerve ligation (SNL: Jiang et al., 2016). CXCR3, as the major receptor of CXCL10, has been shown to be involved in a variety of human diseases, including chronic inflammation, immune dysfunction, cancer, metastasis, and pruritus (Groom and Luster, 2011; Qu et al., 2015; Van Raemdonck et al., 2015). A recent study has shown that CXCR3 deficiency reduced experimental autoimmune encephalomyelitis-evoked hyperalgesia, but did not affect spared nerve injury-induced mechanical allodynia (Schmitz et al., 2013). However, to date, little is known about how the expression of CXCR3 is regulated and whether CXCR3 is involved in SNL-induced neuropathic pain.

DNA methylation involves the transfer of a methyl group to cysteine residues at CpG (cytosine–phosphate–guanine) sites in the promoter regions of genes, a process that plays an important role in regulating gene expression (Bird, 1986). DNA methyltransferases (DNMTs) are important in regulating DNA methylation and can directly inhibit transcription by interfering with transcription factor binding (Poetsch and Plass, 2011; Géranton, 2012). The CCAAT (cytidine–cytidine–adenosine–adenosine–thymidine)/enhancer binding protein α (C/EBPα) is a differentiation-inducing transcription factor that belongs to a family of basic region leucine zipper transcription factors (Koschmieder et al., 2009). C/EBPα promotes the expression of certain genes through interaction with the promoter region. Whether C/EBPα regulates CXCR3 expression and further contributes to neuropathic pain has not previously been elucidated.

In the present study, we investigated how CXCR3 is regulated in the spinal cord in SNL-induced neuropathic pain and how the implied mechanisms involved in such regulation. We found that SNL induced demethylation of the *Cxcr3* gene and increased the binding of C/EBPα with *Cxcr3* promoter. Furthermore, inhibition of CXCR3 by different strategies markedly attenuated neuropathic pain. We also showed that CXCL10 contributed to the maintenance of neuropathic pain via enhanced CXCR3-mediated excitatory synaptic transmission.

Table 1. Primer sets used in qPCR

Gene	Primer sequence	size
Cxcr3	5′-TACCTTGAGGTTAGTGAACGTCA-3′; 5′-CGCTCTCGTTTTCCCCATAATC-3′	100 bp
Cxcl10	5′-TGAATCCGGAATCTAAGACCATCAA-3′; 5′-AGGACTAGCCATCCACTGGGTAAAG-3′	171 bp
Gapdh	5′-AAATGGTGAAGGTCGGTGTGAAC-3′; 5′-CAACAATCTCCACTTTGCCACTG-3′	90 bp

Materials and Methods

Animals and surgery. Adult ICR and C57BL/6 (male, 8 weeks) mice were purchased from the Experimental Animal Center of Nantong University. *Cxcr3* $^{-/-}$ mice (B6.129P2-*Cxcr3* ^{tm1Dgen}/J, stock #005796, RRID:IMSR_JAX:005796) were purchased from the Jackson Laboratory. Female *Cxcr3* ^{tm1Dgen}/J homozygous mice were mated with the C57BL/6 mice to get the F1 heterozygous offspring, and then backcrossed with the *Cxcr3* ^{tm1Dgen}/J homozygous mice to get F2 heterozygous or homozygous offspring. The homozygous and the littermate wild-type (WT) mice were used for experiments. Somatostatin(SST)-Tomato $^{+}$ mice were generated by crossing Sst-IRES-Cre mice (Jackson Laboratory, stock #013044, RRID:IMSR_JAX:013044) with Ai9(RCL-tdT) mice (Jackson Laboratory, stock #007909, RRID:IMSR_JAX:007909). GAD2-Tomato $^{+}$ mice were generated by crossing Gad2-IRES-Cremice (Jackson Laboratory, stock #019022, RRID:IMSR_JAX:019022) with Ai9(RCL-tdT) mice. The animals were maintained in specific-pathogen-free facilities on a 12:12 light/dark cycle at a room temperature of 22 ± 1°C. All animal procedures performed in this study were reviewed and approved by the Animal Care and Use Committee of Nantong University and performed in accordance with the guidelines of the International Association for the Study of Pain. SNL was produced as previously described (Gao et al., 2009). For sham operations, the L5 spinal nerve was exposed but not ligated.

Drugs and administration. Recombinant murine CXCL10 was purchased from PeproTech. A potent and selective CXCR3 antagonist, NBI-74330, was purchased from Tocris Bioscience. Five′-cholesteryl-modified and 2′-O-methyl-modified *Cebpa* small interfering RNA (siRNA; 5′-GGA GTT GAC CAG TGA CAA T3′) and an additional scrambled siRNA were purchased from RiboBio. Intrathecal injection was made with a 30 G needle between the L5 and L6 intervertebral spaces to deliver the reagents to the CSF.

Real-time quantitative PCR. The total RNA of the spinal cord or cultured cells was extracted using Trizol reagent (Invitrogen). One microgram of total RNA was reverse-transcribed using an oligo primer according to the manufacturer's protocol (Takara). Quantitative PCR (qPCR) analysis was performed in a real-time detection system (Rotor-Gene 6000, Qiagen) by SYBR green I dye detection (Takara). The detailed primer sequences for each gene (*Cxcr3, Cxcl10,* and *Gapdh*) are listed in Table 1. The PCR amplifications were performed at 95°C for 30 s, followed by 40 cycles of thermal cycling at 95°C for 5 s and 60°C for 45 s. *Gapdh* was used as an endogenous control to normalize differences. Melt curves were performed on completion of the cycles to ensure that nonspecific products were absent. Quantification was performed by normalizing Ct (cycle threshold) values with *Gapdh* Ct and analyzed with the $2^{-\Delta\Delta CT}$ method.

Bisulfite sequencing PCR. Genomic DNA was extracted using QIAamp DNA Mini Kit (Qiagen) according to the manufacturer's protocol. Sodium bisulfite conversion of genomic DNA was performed using EpiTect Bisulfite Kit (Qiagen). PCR products of genomic DNA fragment-containing promoter amplified from bisulfite-converted genomic DNA using the primers shown in Table 2 were gel-purified with the QIAquick Gel Extraction Kit (Qiagen). The eluted DNA fragments were ligated into

Correspondence should be addressed to Yong-Jing Gao, Institute of Nautical Medicine, Nantong University, 9 Seyuan Road, Nantong, Jiangsu 226019, China. E-mail: gaoyongjing@hotmail.com or gaoyongjing@ntu.edu.cn.
DOI:10.1523/JNEUROSCI.2262-16.2016
 0270-6474/17/370686-16$15.00/0

Table 2. Primer sequences for MSP, BSP, and ChIP experiments

Usage	Primer name	Primer sequence	Size
MSP	*Cxcr3*-M-F	5′-TAAGTGGTCGAGTTCGGATATTA-3′	83 bp
	Cxcr3-M-R	5′-CGATACTACTCACTCAACCCG-3′	
	Cxcr3-U-F	5′-GGTTAAGTGGTTGAGTTTGGATATTA-3′	83 bp
	Cxcr3-U-R	5′-ATTCAATACTACTCACTCAACCCA-3′	
BSP	*Cxcr3*-F	5′-ATTTTTTGGAAGAGGTTGTGTTG-3′	325 bp
	Cxcr3-R	5′-ACTAAATTTCCCAATCCACCAATA-3′	
ChIP	P1-F	5′-TTCCTGGCTAGCCCCTTCTA-3′	169 bp
	P1-R	5′-TTGGCACTTGTGGTTGGGAA-3′	
	P2-F	5′-TGGCTTGGATGCCTCATCTG-3′	118 bp
	P2-R	5′-AATGGGGGCATACCACTTCC-3′	

pGEM-T Easy Vector (Promega) for sequencing. Ten colonies for each mouse were randomly chosen for sequencing.

Methylation-specific PCR. The genomic DNA extraction and bisulfite treatment was performed as described in bisulfite sequencing PCR (BSP). Bisulfite-converted genomic DNA was amplified using the EpiTect Methylation-Specific PCR (MSP) PCR Kit (Qiagen) with methylation-specific or unmethylation-specific primer pairs (Table 2). The PCR products were analyzed by electrophoresis. The percentage of methylation of *Cxcr3* promoter from the spinal cord of SNL and sham-operated animals was determined by densitometric analysis of MSP products (ratio of methylated products to unmethylated products).

Cxcr3 *promoter reporter analysis. Cxcr3* promoter reporter constructs, cloned into the pCpG-free basic reporter vector (InvivoGen), were either methylated or unmethylated by incubation with S-adenosyl methionine in the presence or absence of CpG methylase (M. SssI; Fisher Thermo Scientific). Methylated and unmethylated pCpG-free-*Cxcr3*-Lucia luciferase reporter constructs were transfected into HEK293 (CLS catalog #300192/p777_HEK293, RRID:CVCL_0045) cells using Lipofectamine 3000 (Invitrogen). The activity of secreted coelenterazine luciferase in medium was measured 24 h later with the QUANTI-Luc (InvivoGen) according to the manufacturer's instructions. In brief, 10 μl of medium sample was transferred by pipette to a 96-well white plate, then a 50-μl injector was used to add QUANTI-Luc assay solution. Measurements were performed with a luminometer (Synergy 2 Multi-Mode Reader, BioTEL).

C/EBPα expression vectors were purchased from Obio Technology. C/EBPα expression vectors and methylated or unmethylated pCpG-free-*Cxcr3*-Lucia promoters were transiently transfected into HEK293 cells using Lipofectamine 3000 (Invitrogen). The activity of secreted coelenterazine luciferase in medium was measured 24 h after transfection as described above.

Chromatin immunoprecipitation PCR and quantitative chromatin immunoprecipitation analyses. Chromatin immunoprecipitation (ChIP) assays were performed using the SimpleChIP Enzymatic Chromatin IP kit (Magnetic Beads, Cell Signaling Technology) according to the manufacturer's instructions. After SNL or sham operation, the ipsilateral dorsal horn of the spinal cord was collected and exposed to 1% formaldehyde immediately to cross-link proteins to DNA. After glycine treatment and PBS washing, the tissues were homogenized, the cells were lysed, and the chromatin was harvested and fragmented using enzymatic digestion. The chromatin was then subjected to immunoprecipitation with positive control histone H3 antibody (rabbit, 1:50; Cell Signaling Technology, catalog #4620, RRID:AB_1904005), negative control (NC) normal IgG antibody (rabbit, 1:500; Cell Signaling Technology, catalog #2729, RRID:AB_2617119), C/EBPα antibody (rabbit, 1:100; Santa Cruz Biotechnology, catalog #sc-61X, RRID:AB_631233), and DNMT3b antibody (mouse, 1:250; Abcam, catalog #ab13604, RRID:AB_300494). The complex coprecipitates were captured by protein-G magnetic beads. After immunoprecipitation, the protein–DNA cross-links were reversed and the DNA was purified. The enrichment of the *Cxcr3* promoter sequences were detected by ChIP-PCR and quantitative ChIP-PCR (qChIP-PCR) using the C/EBPα site-specific primer pairs in *Cxcr3* promoter (Table 2). Genomic DNA fragments bound to C/EBPα were analyzed by PCR using random primers (P1 and P2) designed to respectively check C/EBPα binding site 1 and binding sites 2 and 3 in the *Cxcr3* promoter region. Using P2 to check both binding sites 2 and 3 is because C/EBPα binding site 2 is positioned very close to site 3, and no suitable primers to distinguish C/EBPα binding site 2 from binding site 3. Primers for *Dnmt3b* enrichment of DNA sequence were identical to the ones used in C/EBPα ChIP-PCR. ChIP-PCR products were visualized by GelRed (Biotium) staining in 3.0% agarose gels. For qChIP-PCR, DNA samples and standards were analyzed using a LightCycler96 Real-Time PCR System (Roche Diagnostics) and FastStart Essential DNA Green Master for SYBR Green I-based real-time PCR (Roche Diagnostics).

ELISA. Mouse CXCL10 ELISA kit was purchased from R&D Systems. Animals were transcardially perfused with PBS. Spinal cord tissues were homogenized in a lysis buffer containing protease and phosphatase inhibitors (Sigma-Aldrich). For each reaction in a 96-well plate, 100 μg of proteins were used, and ELISA was performed according to the manufacturer's protocol. The standard curve was included in each experiment.

Western blot. Protein samples were prepared in the same way as for ELISA analysis. Protein samples (30 μg) were separated on SDS–PAGE gel and transferred to nitrocellulose blots. The blots were blocked with 5% milk and incubated overnight at 4°C with antibody against CXCR3 (rabbit, 1:200; Boster Biological Technology, catalog #BAO759), DNMT3b (goat, 1:600; Santa Cruz Biotechnology, catalog #sc-10236, RRID:AB_2094128), and pERK (phosphorylated extracellular signal-regulated kinase; 1:500; Cell Signaling Technology, catalog #9101, RRID:AB_331646). For loading control, the blots were incubated with GAPDH antibody (mouse, 1:20,000; Millipore, catalog #MAB374, RRID:AB_2107445). These blots were further incubated with HRP-conjugated secondary antibody, developed in ECL solution, and exposed onto Hyperfilm (Millipore) for 1–5 min. Specific bands were evaluated by apparent molecular size. The intensity of the selected bands was analyzed using ImageJ software (National Institutes of Health, RRID:SCR_003070).

Immunohistochemistry. Animals were deeply anesthetized with isoflurane and perfused through the ascending aorta with PBS followed by 4% paraformaldehyde with 1.5% picric acid in 0.16 M PB. After the perfusion, the L5 spinal cord segment was removed and postfixed in the same fixative overnight. Spinal cord sections (30 μm, free-floating) were cut in a cryostat and processed for immunofluorescence as we described previously (Gao et al., 2009). The sections were first blocked with 5% donkey serum for 2 h at room temperature, then incubated overnight at 4°C with the following primary antibodies: CXCR3 (rabbit, 1: 200; Boster Biological Technology, catalog #BAO759), neurokinin 1 receptor (NK1R; goat, 1:400; Santa Cruz Biotechnology, catalog #sc-14115, RRID:AB_2255736), CXCL10 (goat, 1:100; R&D Systems, catalog #AF-466-NA, RRID:AB_2292487), glial fibrillary acidic protein (GFAP; mouse, 1:5000; Millipore, catalog #MAB360, RRID:AB_2275415), NeuN (mouse, 1:1000; Millipore, catalog #MAB377, RRID:AB_2298772), IBA-1 (rabbit, 1:3000; Wako, catalog #019-19741, RRID:AB_839504), CD11b (mouse, 1:100; Serotec, catalog #MCA-257GA, RRID:AB_566455), C/EBPα (rabbit, 1:400; Boster Biological Technology, catalog #BAO669), pERK (rabbit, 1:500; Cell Signaling Technology, catalog #9101, RRID:AB_331646). The sections were then incubated for 1 h at room temperature with Cy3-conjugated or FITC-conjugated secondary antibodies (1:400; Jackson ImmunoResearch). For double immunofluorescence, sections were incubated with a mixture of different primary antibodies followed by a mixture of FITC-conjugated and Cy3-conjugated secondary antibodies. The stained sections were examined with a Leica fluorescence microscope, and images were captured with a CCD Spot camera.

In situ *detection of* Cxcr3 *mRNA.* Digoxigenin (DIG)-labeled RNA antisense and sense probes for the *Cxcr3* gene were produced using PCR and *in vitro* transcription with a DIG RNA Labeling Kit (SP6/T7; Roche Diagnostics). The template fragments were amplified using a set of primers (forward: 5′-AAC AGC ACC TCT CCC TAC GA-3′ and reverse: 5′-CAG CCA CTA GCT GCA GTA CA-3′) and then subcloned into pSPT18. Cellular localization of *Cxcr3* was performed using a mouse *Cxcr3* mRNA *in situ* hybridization assay kit (Boster Biological Technology) as described previously (Zhang et al., 2013). Briefly, *in situ* hybridizations were performed in 14 μm cryosections from the spinal cord. Sections were fixed in 4% paraformaldehyde/0.1 M PBS for 30 min followed by washes in DEPC-treated ultrapure water. Prehybridization procedures

were performed under RNase-free conditions for 4 h at room temperature. Hybridization was performed with a hybridization probe specific to *Cxcr3* at 42°C overnight in hybridization buffer. Sections were then incubated in blocking solution at 37°C for 30 min and in mouse anti-DIG-biotin for 60 min, washed, incubated using streptavitin–biotin complex-FITC reagent (Boster Biological Technology, SA1080) for 30 min.

To identify the cell types expressing *Cxcr3* and colocalization of *Cxcr3* with C/EBPα, the above sections under *in situ* hybridization were incubated overnight at 4°C with primary antibodies against GFAP (mouse, 1:6000; Millipore, catalog #MAB360, RRID:AB_2275415), NeuN (mouse, 1:1000; Millipore, catalog #MAB377, RRID:AB_2298772), IBA-1 (rabbit, 1:3000; Wako, catalog #019-19741, RRID:AB_839504), and C/EBPα (rabbit, 1:400; Boster Biological Technology, catalog #BAO669). On the following day, Cy3-conjugated secondary antibody was added and incubated for 2 h. The signal was detected with a Leica SP8 gated stimulated emission depletion confocal microscope (Leica Microsystems).

Lentiviral vectors production and intraspinal injection. The shRNA targeting the sequence of mice *Cxcr3* (Gene Bank Accession: NM_009910.2) was designed. An additional scrambled sequence was also designed as an NC. The recombinant lentivirus containing *Cxcr3* shRNA (LV-*Cxcr3* shRNA, 5′-CTG AAC TTT GAC AGA ACC T-3′) or NC shRNA (LV-NC, 5′-TTC TCC GAA CGT GTC ACG T-3′) was packaged using pGCSIL-GFP vector by Shanghai GeneChem. To test the knock-down effect, the *Cxcr3*-expressing plasmid and *Cxcr3* shRNA plasmid were transfected to HEK293 cells. Two days after transfection, the cells were harvested and subjected to quantitative real-time PCR (RT-PCR). The coding sequences of *Dnmt3b* (GenBank Accession: NM_001122997.2) were synthesized by Sangon Biotech and cloned into pLV-Ubi-MCS-3FLAG to generate *Dnmt3b*-expressing lentiviral plasmid, which mediated transcription of *Dnmt3b* by ubiquitin promoter. Then the *Dnmt3b*-expressing plasmid and EGFP-expressing plasmid (control) were packaged into lentivirus. The intraspinal injection was performed as described previously (Zhang et al., 2013).

Behavioral analysis. Animals were habituated to the testing environment daily for ≥2 d before baseline testing. All the behavioral experiments were done by individuals blinded to the treatment or genotypes of the mice. For heat hyperalgesia, the animals were put in a plastic box placed on a glass plate, and the plantar surface was exposed to a beam of radiant heat through a transparent glass surface (IITC model 390 Analgesia Meter, Life Science). The baseline latencies were adjusted to 12–15 s with a maximum of 20 s as cutoff to prevent potential injury (Hargreaves et al., 1988). For mechanical allodynia, the animals were put in boxes on an elevated metal mesh floor and allowed 30 min for habituation before examination. The plantar surface of the hindpaw was stimulated with a series of von Frey hairs with logarithmically incrementing stiffness (0.02–2.56 g, Stoelting). The 50% paw-withdrawal threshold was determined using Dixon's up–down method (Dixon, 1980). For the tail-immersion test, the temperature of the water was set at 48, 50, or 52°C. The tail-flick latency was recorded (Ramabadran et al., 1989). For the rotarod test, the speed was set at 10 rpm for 60 s and subsequently accelerated to 80 rpm in 5 min. The time taken for mice to fall after the beginning of the acceleration was recorded (Abbadie et al., 2003).

Spinal slice preparation. The lumbar spinal cord was carefully removed from mice (4–6 weeks) under urethane anesthesia (1.5~2 g/kg, i.p.) and placed in preoxygenated (saturated with 95% O_2 and 5% CO_2) ice-cold sucrose artificial CSF (aCSF) solution. The sucrose aCSF contained the following (in mM): 234 sucrose, 3.6 KCl, 1.2 $MgCl_2$, 2.5 $CaCl_2$, 1.2 NaH_2PO_4, 12 glucose, and 25 $NaHCO_3$. The pia-arachnoid membrane was gently removed from the section. The portion of the lumbar spinal cord (L4–L5) was identified by the lumbar enlargement and large dorsal roots. The spinal segment was placed in a shallow groove formed in an agar block and then glued to the button stage of a VT1000S vibratome (Leica). Transverse slices (450 μm) were cut in the ice-cold sucrose aCSF, incubated in Krebs' solution oxygenated with 95% O_2 and 5% CO_2 at 34°C for 30 min, and then allowed to recover 1~2 h at room temperature before the experiment. The Krebs' solution contained the following (in mM): 117 NaCl, 3.6 KCl, 1.2 $MgCl_2$, 2.5 $CaCl_2$, 1.2 NaH_2PO_4, 25 $NaHCO_3$, and 11 glucose.

Patch-clamp recordings in spinal slices. The voltage-clamp recordings were made from neurons in outer lamina II of the dorsal horn. The slice was continuously superfused (3–5 ml/min) with Krebs' solution in room temperature, and saturated with 95% O_2 and 5% CO_2. Individual neurons were visualized under a stage-fixed upright infrared differential interference contrast microscope (BX51WI, Olympus) equipped with a 40× water-immersion objective. The patch pipettes were pulled using a Flaming micropipette puller (P-97, Sutter Instruments), and had initial resistance of 5~10 MΩ when filled with the internal pipette solution contained the following (in mM): 135 potassium gluconate, 5 KCl, 0.5 $CaCl_2$, 2 $MgCl_2$, 5 EGTA, 5 HEPES, and 5 Na_2ATP. Membrane voltage and current were amplified with a multiclamp 700B amplifier (Molecular Devices). Data were filtered at 2 kHz and digitized at 10 kHz using a data acquisition interface (1440A, Molecular Devices). A seal resistance (>2 GΩ) and an access resistance (<35 MΩ) were considered acceptable. The cell capacity transients were cancelled by the capacitive cancelation circuitry on the amplifier. After establishing the whole-cell configuration, the membrane potential was held at −70 mV for recording sEPSCs. NMDA-induced or AMPA-induced current was recorded by puff application of NMDA (50 μM; Sigma-Aldrich) or AMPA (10 μM, Sigma-Aldrich) at the holding potential of −45 and −70 mV, respectively. Data were stored with a personal computer using pClamp10.0 software and analyzed with Mini Analysis (Synaptosoft 6.0). Those cells that showed >10% changes from the baseline levels were regarded as responsive to the presence of drugs.

Quantification and statistics. All data were expressed as mean ± SEM. The behavioral data were analyzed by two-way repeated-measures ANOVA followed by Bonferroni's test as the *post hoc* multiple-comparison analysis. For Western blot, the density of specific bands was measured with ImageJ. The levels of CXCR3, DNMT3b, C/EBPα, and pERK were normalized to loading control GAPDH. Differences between groups were compared using one-way ANOVA followed by Bonferroni's test. Student's *t* test was applied when only two groups needed to be compared. The criterion for statistical significance was $p < 0.05$.

Results

CXCR3 expression is upregulated in spinal neurons after SNL

SNL induces rapid (1 d) and persistent (>21 d) mechanical allodynia and heat hyperalgesia (Zhang et al., 2013). We first examined *Cxcr3* expression in the spinal cord at days 1, 3, 10, and 21 after SNL. SNL induced persistent *Cxcr3* mRNA upregulation, which started at day 3, peaked at day 10, and was still elevated at day 21 (Fig. 1*A*). CXCR3 protein level was also significantly increased 10 d after SNL (Fig. 1*B*). Immunostaining revealed basal expression of CXCR3 in the dorsal horn in naive mice (Fig. 1*C*). CXCR3 immunoreactivity was markedly increased in the ipsilateral dorsal horn (Fig. 1*D*), but not in the contralateral dorsal horn (Fig. 1*E*) 10 d after SNL.

To define the cellular localization of CXCR3 in the spinal cord, we performed *in situ* hybridization using antisense probes for *Cxcr3* on spinal sections 10 d after SNL. A *Cxcr3*-positive signal was not evident in sections incubated with the *Cxcr3* sense probe (Fig. 1*F*), but was obvious in sections with the antisense probe (Fig. 1*G*,*H*). *In situ* hybridization combined with immunostaining showed that *Cxcr3* mRNA was highly colocalized with neuronal marker NeuN (Fig. 1*I*), partially colocalized with microglial marker IBA-1 (Fig. 1*J*), but not at all colocalized with astrocytic marker GFAP (Fig. 1*K*), suggesting the predominant expression of *Cxcr3* by spinal neurons.

We further characterized the type of CXCR3$^+$ neurons. NK1R is expressed by ~80% of ascending projection neurons in lamina I (Todd, 2010). Double staining of NK1R and CXCR3 showed that CXCR3 was expressed in NK1R-positive neurons in lamina I (Fig. 1*L*). As SST and GAD2 are respectively expressed in excitatory and inhibitory neurons (Zeilhofer et al., 2012; Duan et al., 2014), we performed CXCR3 staining on SST-Tomato$^+$ or GAD2-Tomato$^+$ mice. It showed that both SST-Tomato$^+$ neurons and GAD2-

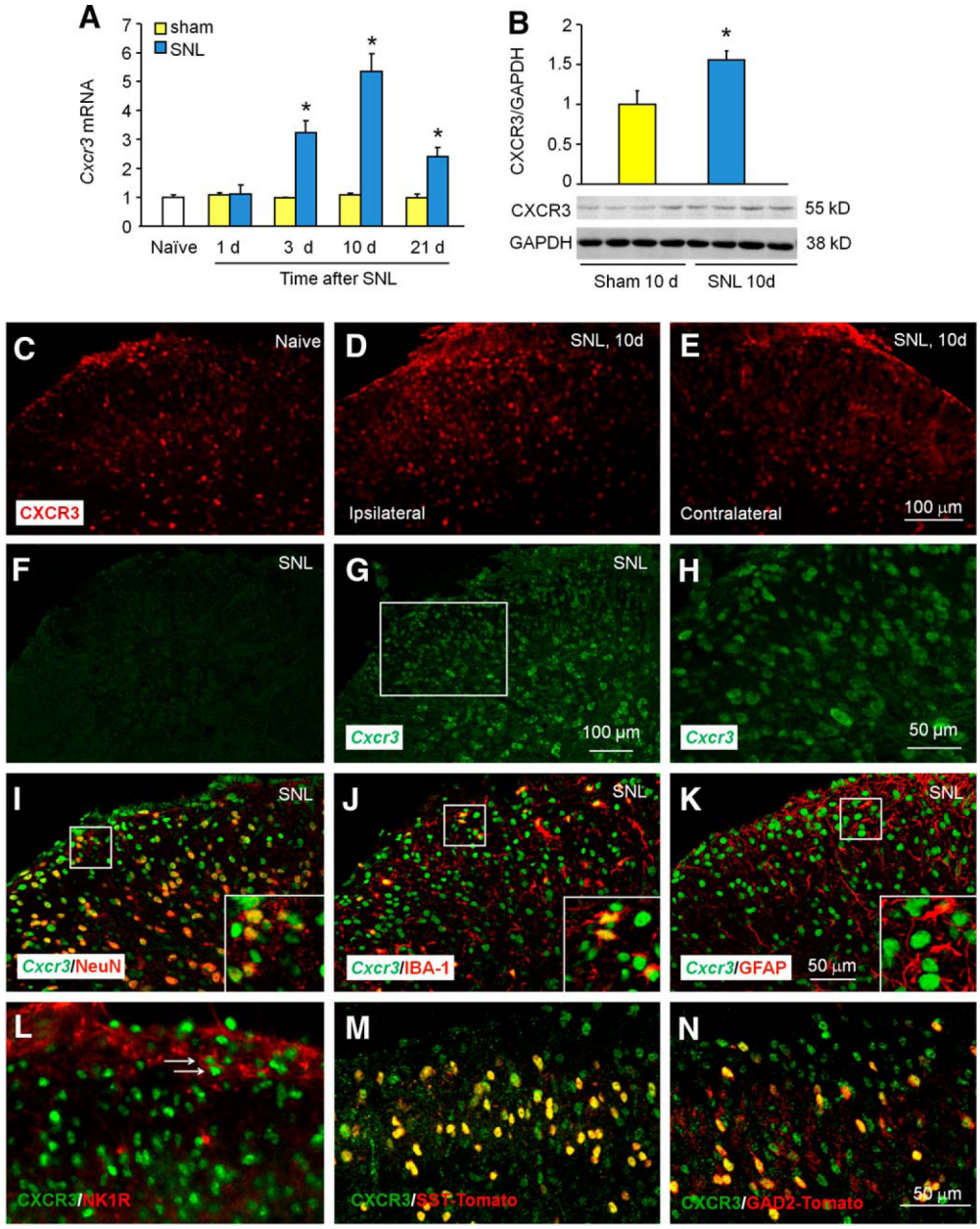

Figure 1. CXCR3 expression is increased mainly in spinal neurons after SNL. ***A***, Time course of *Cxcr3* mRNA expression in the ipsilateral dorsal horn in naive, sham-operated, and SNL mice. *Cxcr3* expression at 3, 10, and 21 d increased more in SNL mice than in sham-operated mice. *$p < 0.05$, Student's *t* test. $n = 4–5$ mice/group. ***B***, Western blotting shows the increase of CXCR3 protein in the spinal cord 10 d after SNL. *$p < 0.05$, Student's *t* test, $n = 4$ mice/group. ***C–E***, Representative images of CXCR3 immunofluorescence in the spinal cord from naive and SNL mice. CXCR3 was constitutively expressed in naive mice (***C***), remarkably increased in the ipsilateral dorsal horn of SNL mice (***D***), but not in the contralateral side (***E***). ***F–H***, *In situ* hybridization of *Cxcr3* mRNA shows that no signals were found in spinal sections incubated with *Cxcr3* sense probe (***F***), but positive signals were apparent in sections incubated with antisense probe (***G***, ***H***). ***H***, High-magnification image of ***G***. ***I–K***, *In situ* hybridization of *Cxcr3* mRNA and immunofluorescence staining of NeuN (***I***), IBA-1 (***J***), and GFAP (***K***) shows that *Cxcr3* mRNA was predominantly colocalized with neuronal marker NeuN, rarely with microglia marker IBA-1, and not at all with astrocyte marker GFAP. ***L***, Double staining of NK1R and CXCR3 in the spinal dorsal horn. ***M***, ***N***, Immunofluorescence staining of CXCR3 on the spinal cord from SST-Tomato$^+$ (***M***) and GAD2-Tomato$^+$ (***N***) mice 10 d after SNL.

Tomato$^+$ neurons can express CXCR3, and the percentages of these neurons in CXCR3$^+$ cells were 57 ± 2% and 32 ± 1%, respectively, in laminae I–IV (Fig. 1*M*,*N*). These data suggest that CXCR3 is widely distributed in all three populations of neurons.

Demethylation of the CpG sites of the *Cxcr3* gene promoter region after SNL

DNA methylation is an important epigenetic mechanism controlling gene expression (Jaenisch and Bird, 2003). To determine whether DNA methylation contributes to *Cxcr3* upregulation, we examined the methylation status of the *Cxcr3* promoter region by MSP and BSP assays. The genomic structure of the *Cxcr3* gene contains one CpG dinucleotide region with nine CpG sites around the transcriptional starting site (TSS; Fig. 2*A*). The MSP assay showed that the methylation degree of *Cxcr3* promoter in the spinal cord of SNL mice was lower than that in sham-operated mice (Fig. 2*B*). To further confirm the methylation status of the nine CpG sites within *Cxcr3* promoter, DNA sequencing was performed on PCR products of the 325 bp fragment obtained after the treatment of genomic DNA samples with sodium bisulfite. As shown in Figure 2*C*, all spinal cord samples were successfully sequenced. Consistent with the MSP assay, DNA methylation in CpG dinucleotide regions of the

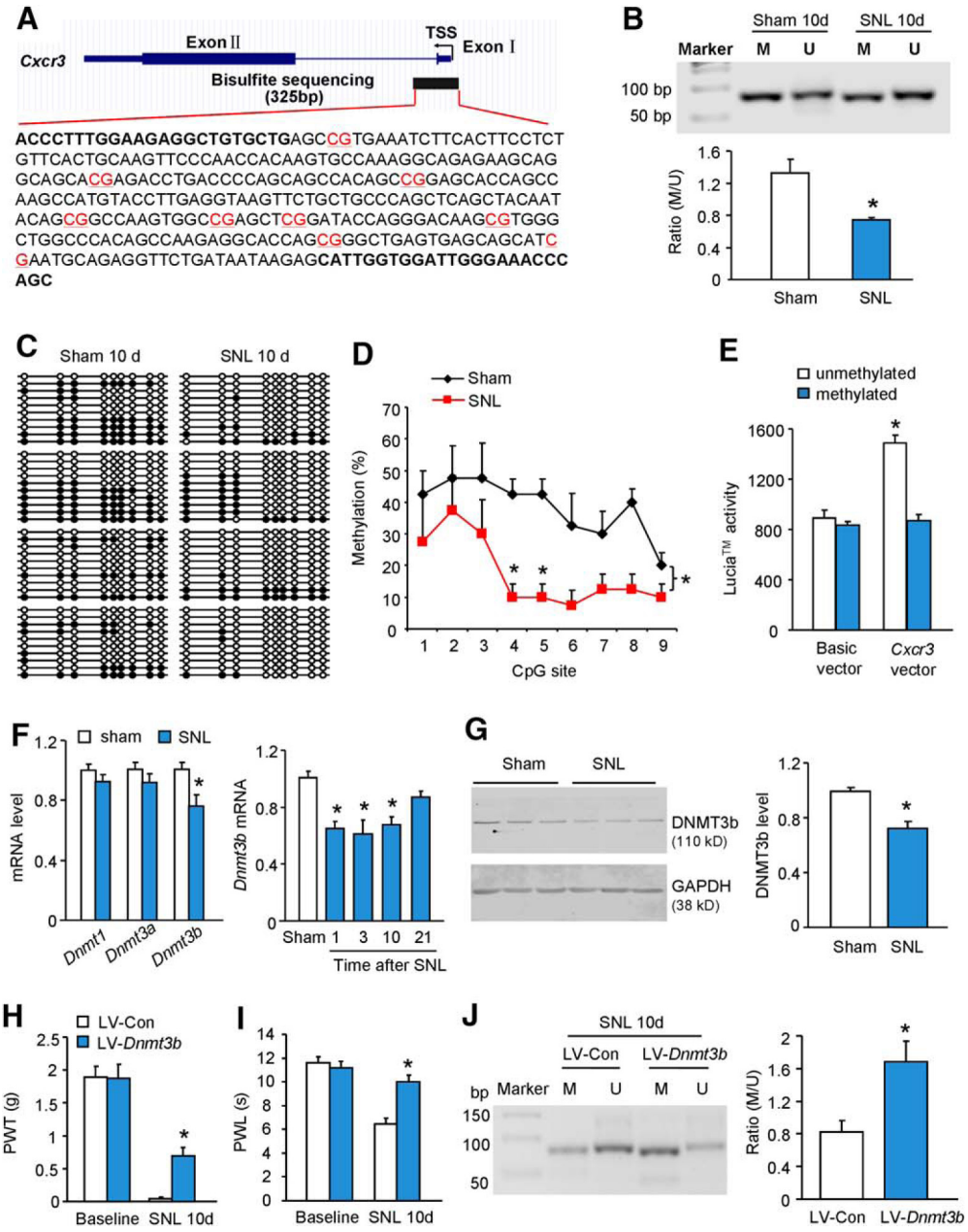

Figure 2. Demethylation of *Cxcr3* gene promoter region after SNL. ***A***, Schematic of a CpG island showing the locations of the nine CpG sites (in red) in the *Cxcr3* gene promoter area. ***B***, Representative PCR results of the *Cxcr3* promoter region using primers for methylation-specific or unmethylation-specific amplifications of genomic DNA from the spinal cord of sham-operated or SNL-operated mice. SNL reduced the ratio of methylated (M) to unmethylated (U) products of CpG sites. $*p < 0.05$, SNL versus sham, Student's *t* test, $n = 3$ mice/group. ***C***, Bisulfite sequencing data of *Cxcr3* promoter of spinal dorsal horn from SNL ($n = 4$) and sham-operated ($n = 4$) mice. Ten clones were randomly collected from each mouse. Filled circles, Methylated CpG sites; unfilled circles, unmethylated CpG sites. ***D***, Overall methylation of *Cxcr3* promoter was decreased in SNL mice. $*p < 0.05$, SNL versus sham, two-way ANOVA, $n = 4$ mice/group. ***E***, Luciferases assay using coelenterazine shows that the luciferase activity was increased when HEK293 cells were transfected with unmethylated pCpG-free-*Cxcr3*-promoter-Lucia vector compared with that transfected with methylated pCpG-free-*Cxcr3*-promoter-Lucia vector. $*p < 0.05$, unmethylated versus methylated, $n = 3$/group. ***F***, *Dnmt1* mRNA and *Dnmt3a* mRNA were not changed 10 d after SNL. However, *Dnmt3b* mRNA level decreased at days 1, 3, and 10 after SNL. $*p < 0.05$, one-way ANOVA, $n = 5–6$ mice/group. ***G***, DNMT3b protein was decreased in the spinal cord 10 d after SNL. $*p < 0.05$, Student's *t* test, $n = 3$ mice/group. ***H***, ***I***, Intraspinal injection of LV-*Dnmt3b*, 7 d before SNL, attenuated SNL-induced mechanical allodynia (***H***) and heat hyperalgesia (***I***). $*p < 0.05$, LV-*Dnmt3b* versus LV-Con, two-way repeated-measures ANOVA followed by Bonferroni's tests, $n = 7$ mice/group. ***J***, Pretreatment with LV-*Dnmt3b* increased the methylation of *Cxcr3* promoter in the spinal cord 10 d after SNL. $*p < 0.05$, LV-*Dnmt3b* vs LV-Con, Student's *t* test, $n = 4–6$ mice/group.

Cxcr3 gene was less in SNL mice compared with sham-operated mice (Fig. 2*D*).

The effect of DNA methylation on *Cxcr3* promoter activity was further analyzed in an *in vitro* cell culture system using a luciferase assay employing coelenterazine. The luciferase activity was not different between transfection with methylated pCpG-free and unmethylated pCpG-free basic reporter vector in HEK293 cells (Fig. 2*E*). However, luciferase activity for cells transfected with unmethylated pCpG-free-*Cxcr3*-promoter-Lucia vector was more than that of cells transfected with methylated pCpG-free-*Cxcr3*-promoter-Lucia vector (Fig. 2*E*), indicating that the promoter activity of the mouse *Cxcr3* gene is increased by DNA demethylation.

Knowing that DNMTs are important in directly regulating DNA methylation (Jurkowska et al., 2011), we then examined the

expression of three *Dnmts*: *Dnmt1*, *Dnmt3a*, and *Dnmt3b* in the spinal cord 10 d after SNL. As shown in Figure 2*F*, *Dnmt3b*, but not *Dnmt1* or *Dnmt3a*, decreased in the spinal cord after SNL. The time course of *Dnmt3b* mRNA expression showed that the *Dnmt3b* level was reduced at days 1, 3, and 10 (Fig. 2*F*). DNMT3b protein was also remarkably decreased in the spinal cord after SNL (Fig. 2*G*). These data suggest that downregulated DNMT3b may be responsible for the demethylation of *Cxcr3* promoter in neuropathic pain condition.

To check whether DNMT3b could directly regulate *Cxcr3* methylation, we intraspinally injected *Dnmt3b*-expressing lentivirus (LV-*Dnmt3b*) and control lentivirus (LV-Con). Seven days after injection, LV-*Dnmt3b* effectively increased *Dnmt3b* mRNA expression by 10.7 ± 2.2-fold ($p < 0.05$, vs LV-Con, $n = 7$ mice per group) in the spinal cord. In addition, injection of LV-*Dnmt3b* 7 d before SNL significantly alleviated SNL-induced mechanical allodynia (Fig. 2*H*) and heat hyperalgesia (Fig. 2*I*), besides increasing the methylation of *Cxcr3* promoter in the spinal cord 10 d after SNL (Fig. 2*J*). These data confirmed the regulation of DNMT3b on *Cxcr3* methylation and the involvement of DNMT3b in the pathogenesis of neuropathic pain.

Increased binding of C/EBPα with *Cxcr3* gene promoter is associated with decreased binding of DNMT3b with *Cxcr3* gene promoter after SNL

DNA methylation can regulate transcription by interfering with transcription factor binding (Poetsch and Plass, 2011). To reveal the transcriptional factor that may regulate *Cxcr3* expression, the sequence from −1500 to +500 of *Cxcr3* promoter was analyzed. Three C/EBPα binding sites (site 1: at 4–14 from TSS; site 2: at 256–267 from TSS; site 3: at 337–347 from TSS; Fig. 3*A*) were predicted within the *Cxcr3* promoter region based on Core vertebrata Jaspar matrix models with a defined 80% profile score threshold (http://jaspar.genereg.net/). A conservation analysis using the University of California Santa Cruz genome browser showed that sites 1 and 2, but not site 3, are well conserved among mice, rats, and humans (data not shown).

To determine the effect of C/EBPα on *Cxcr3* expression, we conducted a luciferase activity assay in HEK293 cells. C/EBPα-expressing vector and pCpG-free-*Cxcr3*-promoter-Lucia vector (methylated or unmethylated) were cotransfected. As shown in Figure 3*B*, in HEK293 cells transfected with methylated pCpG-free-*Cxcr3*-promoter-Lucia vector, cotransfection of C/EBPα-expressing vectors slightly increased the promoter luciferase activity, compared with absence of C/EBPα-expressing vector. However, in HEK293 cells transfected with unmethylated pCpG-free-*Cxcr3*-promoter-Lucia vector, cotransfection of C/EBPα-expressing vector dramatically increased the luciferase activity, compared with absence of C/EBPα-expressing vector. In addition, C/EBPα induced more luciferase activity increase in cells transfected with unmethylated pCpG-free-*Cxcr3*-promoter-Lucia vector than in cells transfected with methylated pCpG-free-*Cxcr3*-promoter-Lucia vector (Fig. 3*B*). These results suggest that C/EBPα can increase the transcription of the *Cxcr3* gene and that this increase is further enhanced when *Cxcr3* promoter is demethylated.

We then examined the binding of C/EBPα with *Cxcr3* promoter in the spinal cord after SNL by ChIP-PCR. After C/EBPα antibody immunoprecipitation, the DNA fragments amplified by primer pairs either P1 (primers for site 1) or P2 (primers for sites 2 and 3) were increased in the spinal cord of SNL mice compared with sham-operated mice (Fig. 3*C*), indicating that the binding of C/EBPα with *Cxcr3* promoter in the spinal cord is specific and also enhanced by SNL.

To further check whether the increased binding of C/EBPα with *Cxcr3* promoter is associated with the decreased binding of DNMT3b with *Cxcr3* promoter, we examined the binding of *Dnmt3b* with *Cxcr3* in the same binding regions of C/EBPα with *Cxcr3* promoter. ChIP-PCR using primers P2, but not P1, revealed that the binding of DNMT3b to *Cxcr3* promoter regions was decreased in SNL mice compared with sham-operated mice (Fig. 3*D*). These data suggest that the decreased binding of DNMT3b with *Cxcr3* promoter at binding sites 2 and 3 demethylates *Cxcr3* promoter and further facilitates the binding of C/EBPα with *Cxcr3* promoter.

Cebpa siRNA attenuates SNL-induced pain hypersensitivity and decreases *Cxcr3* expression in the spinal cord

We then examined C/EBPα expression in the spinal cord after SNL. RT-PCR showed that *Cebpa* mRNA was significantly increased at days 3, 10, and 21 after SNL (Fig. 3*E*). Western blot further confirmed the increase of C/EBPα protein 10 d after SNL (Fig. 3*F*). Immunofluorescence staining combined with *in situ* hybridization showed that C/EBPα was highly colocalized with *Cxcr3* mRNA 10 d after SNL (Fig. 3*G*), supporting the regulation of C/EBPα on CXCR3 in spinal neurons.

To determine whether C/EBPα plays a role in the development of SNL-induced neuropathic pain, we intrathecally injected *Cebpa* siRNA 1 d before SNL. Behavioral data showed that *Cebpa* siRNA dramatically increased the paw-withdrawal threshold, compared with NC-injected mice, 2 and 3 d after SNL, but this effect was insignificant at day 4 (Fig. 3*H*). Meanwhile, *Cebpa* siRNA also attenuated SNL-induced heat hyperalgesia at days 2 and 3 (Fig. 3*I*). To confirm the knock-down effect of *Cebpa* siRNA, we checked mRNA level in another sets of animals 3 d after SNL. As shown in Figure 3*J*, *Cebpa* siRNA significantly reduced *Cebpa* mRNA expression and also reduced *Cxcr3* mRNA expression in the spinal cord.

To check whether CEBP/α is involved in the maintenance of neuropathic pain, we intrathecally injected *Cebpa* siRNA 10 d after SNL. As shown in Figure 3*K*,*L*, *Cebpa* siRNA attenuated both mechanical allodynia (Fig. 3*K*) and heat hyperalgesia (Fig. 3*L*) at 1 and 2 d postinjection. The same treatment also reduced the expression of *Cebpa* mRNA and *Cxcr3* mRNA (Fig. 3*M*). These results suggest that C/EBPα regulates CXCR3 expression and is involved in SNL-induced neuropathic pain.

Deletion or inhibition of CXCR3 persistently attenuates SNL-induced pain hypersensitivity

To determine the role of CXCR3 in pain sensation, we first examined whether acute pain or neuropathic pain are changed in *Cxcr3* knock-out (KO; *Cxcr3*$^{-/-}$) mice. Acute thermal sensitivity tested by hot-water immersion (Fig. 4*A*) and radiant heat (Fig. 4*B*) were indistinguishable in WT and *Cxcr3*$^{-/-}$ mice. Acute mechanical sensitivity was not different between the two genotypes either (Fig. 4*C*). The rotarod test revealed a similar falling latency in WT and *Cxcr3*$^{-/-}$ mice (Fig. 4*D*). These data indicate that *Cxcr3* deletion did not cause deficits in acute pain sensation and motor function. Consistently, *Cxcr3*$^{-/-}$ mice show normal distribution patterns of the neurochemical markers NeuN and PKCγ, astrocyte marker GFAP, and microglia marker IBA-1. The mice also show normal innervations of the primary afferents, labeled with CGRP and IB4 in the spinal cord dorsal horn (Fig. 4*E–P*).

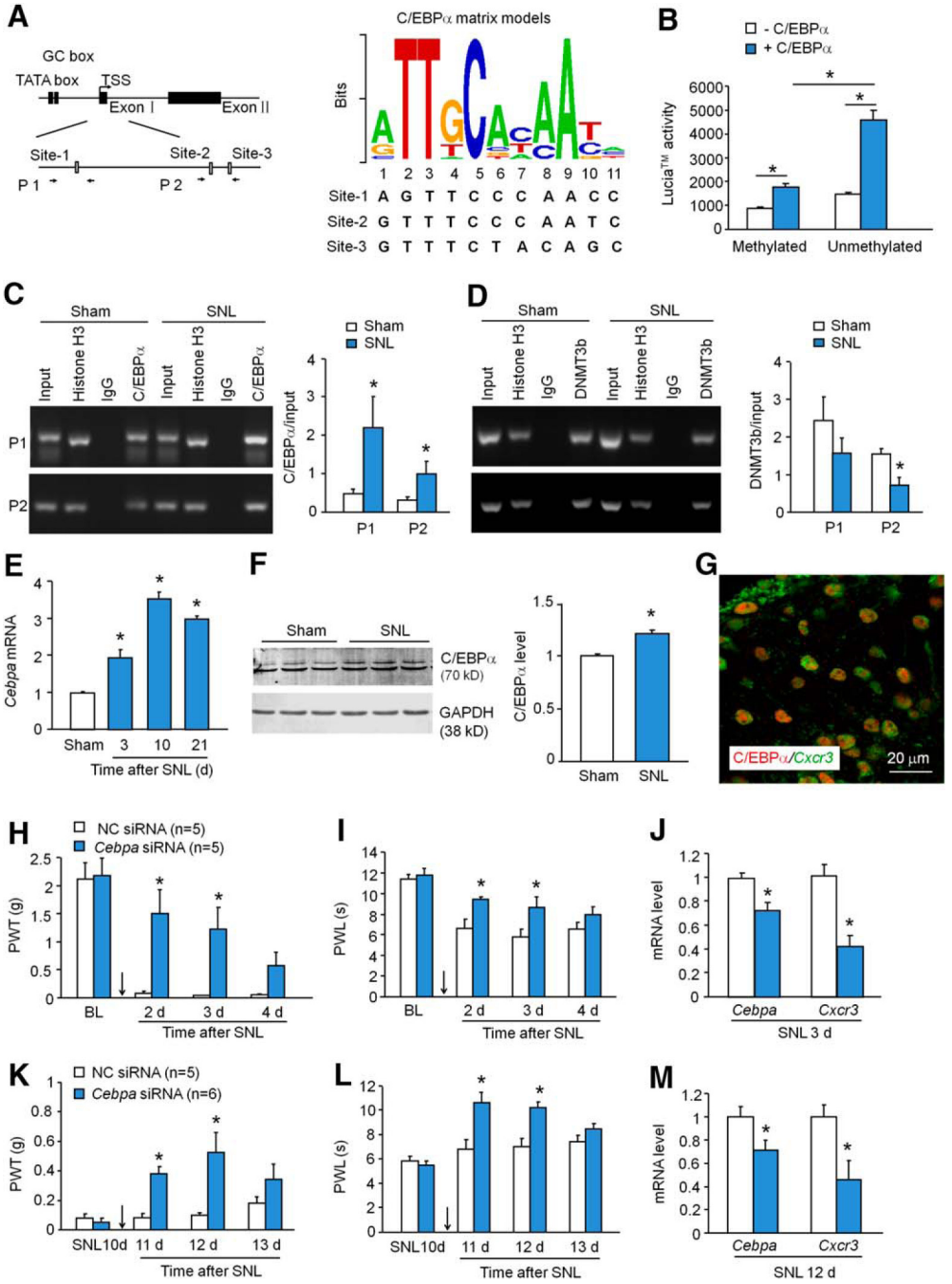

Figure 3. C/EBPα increases CXCR3 expression in the spinal cord after SNL. ***A***, Schematic of *Cxcr3* gene promoter showing locations of the three binding sites for C/EBPα with *Cxcr3* within the CpG islands (left). P1 and P2 were ChIP-PCR primer pairs. Right, The logos of the standard C/EBPα motif and three predicted C/EBPα binding sites in *Cxcr3* gene promoter. ***B***, Cotransfection of C/EBPα-expressing vector with unmethylated pCpG-free-*Cxcr3*-promoter-Lucia vector dramatically increased the luciferase activity. $*p < 0.05$, two-way ANOVA. ***C***, ChIP assay shows the increased binding of C/EBPα with the binding sites 1 and 2 at *Cxcr3* promoter after SNL. $*p < 0.05$, Student's *t* test, $n = 5–6$ mice/group. ***D***, The binding of DMNT3b with *Cxcr3* promoter on the binding site 2 was decreased after SNL. $*p < 0.05$, Student's *t* test, $n = 4$ mice/group. ***E***, *Cebpa* mRNA expression was increased at days 3, 10, and 21 after SNL. $p < 0.05$, one-way ANOVA, $n = 3$ mice/group. ***F***, C/EBPα protein was increased 3 d in the spinal cord after SNL. $p < 0.05$, Student's *t* test. ***G***, Immunofluorescence staining of C/EBPα and *in situ* hybridization of *Cxcr3* mRNA shows that C/EBPα was highly colocalized with *Cxcr3* in the spinal cord dorsal horn 10 d after SNL. ***H***, ***I***, Intrathecal injection of C/EBPα siRNA 1 d before SNL attenuated SNL-induced mechanical allodynia (***H***) and heat hyperalgesia (***I***) for 2 d. $*p < 0.05$, two-way repeated-measures ANOVA followed by Bonferroni's tests. ***J***, Pretreatment with *Cebpa* siRNA reduced the expression of *Cebpa* mRNA and *Cxcr3* mRNA in the spinal cord 2 d after SNL. $*p < 0.05$, Student's *t* test, $n = 5$ mice/group. ***K–M***, Intrathecal injection of C/EBPα siRNA 10 d after SNL attenuated mechanical allodynia (***K***) and heat hyperalgesia (***L***), and also reduced mRNA expression of *Cebpa* and *Cxcr3* in the spinal cord (***M***). $*p < 0.05$, $n = 5–6$ mice/group.

Next, we tested pain behaviors after SNL. Consistent with previous reports (Jiang et al., 2016), SNL induced persistent mechanical allodynia (Fig. 5*A*) and heat hyperalgesia (Fig. 5*B*) in WT mice. However, SNL-induced mechanical allodynia was substantially reduced in *Cxcr3*$^{-/-}$ mice from 3 to 28 d (Fig. 5*A*). In addition, heat hyperalgesia was also markedly reduced in *Cxcr3*$^{-/-}$ mice at 28 d (Fig. 5*B*).

To further investigate the role of spinal CXCR3 in the maintenance of neuropathic pain, we intraspinally injected *Cxcr3* shRNA lentivirus (LV-*Cxcr3* shRNA) and LV-NC 5 d after SNL in

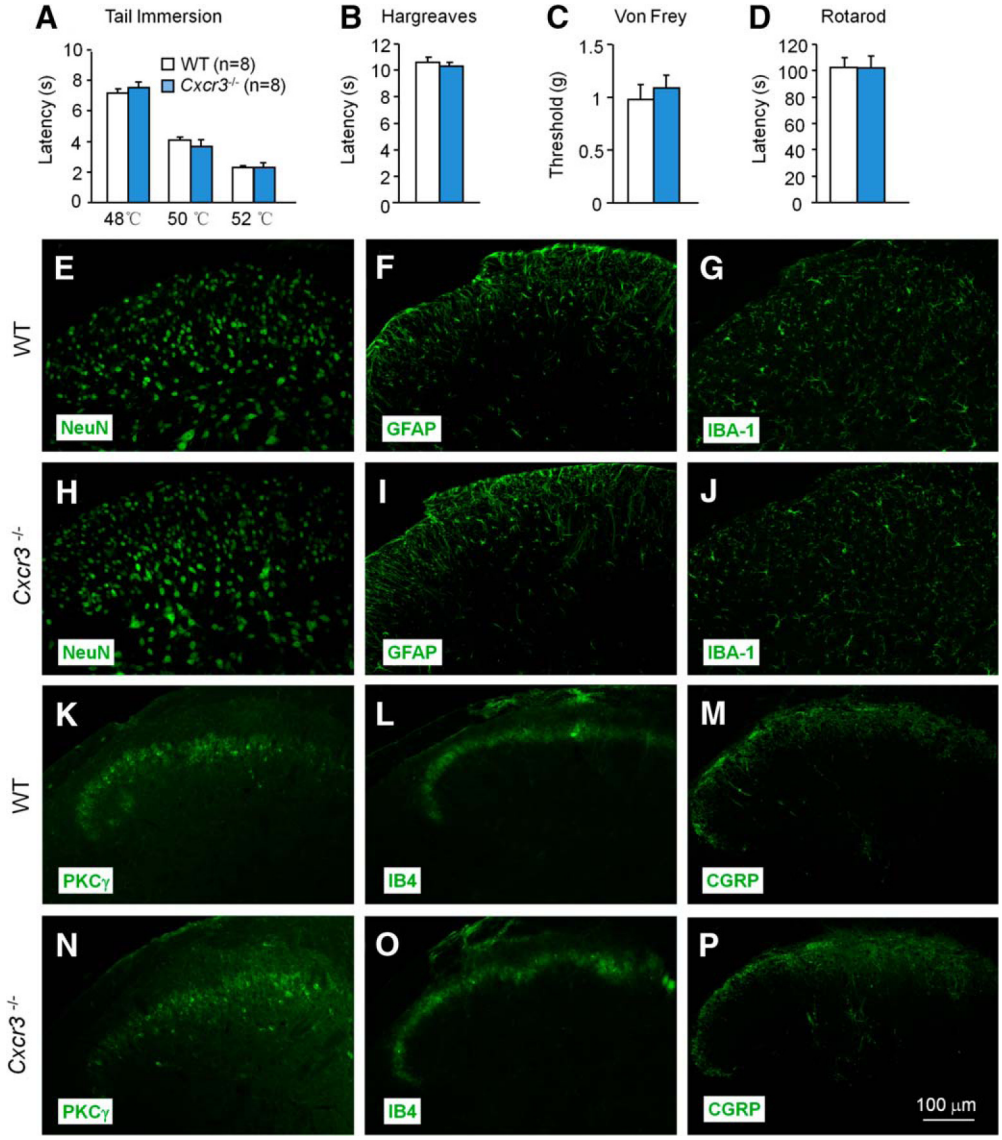

Figure 4. *Cxcr3* KO mice are normal in basal pain and in the expression of cellular markers and neurochemical markers. ***A–D***, *Cxcr3* KO mice show normal acute pain threshold and motor function. Acute pain thresholds tested by tail immersion (***A***), Hargreaves test (***B***), and von Frey test (***C***). ***D***, Motor function assessed by recording the falling latency on a rotarod. ***E–P***, The distribution of the cellular marker NeuN (***E***, ***H***), GFAP (***F***, ***I***), and IBA-1(***G***, ***J***), and of neurochemical markers PKCγ (***K***, ***N***), IB4 (***L***, ***O***), and CGRP (***M***, ***P***) in the spinal dorsal horn of WT and *Cxcr3* KO mice.

WT mice. An *in vitro* study in HEK293 cells showed that LV-*Cxcr3* shRNA reduced *Cxcr3* expression by 87.0 ± 0.5% compared with LV-NC ($p < 0.05$, $n = 4$). Intraspinal injection of LV-*Cxcr3* shRNA attenuated SNL-induced mechanical allodynia from 10 to 28 d after SNL (Fig. 5*C*). LV-*Cxcr3* shRNA also reversed SNL-induced heat hyperalgesia (Fig. 5*D*). qPCR data showed that spinal injection of LV-*Cxcr3* shRNA reduced *Cxcr3* mRNA expression in lumbar segments by 82.9 ± 12.7% compared with LV-NC 21 d after SNL ($p < 0.05$, $n = 3$), confirming the knock-down effect of LV-*Cxcr3* shRNA.

To further check whether a single bolus injection of CXCR3 antagonist could attenuate established neuropathic pain, NBI-74330, a potent and selective CXCR3 antagonist, was intrathecally injected 10 d after SNL. NBI-74330 at the dose of 20 μg significantly attenuated the threshold at 1 and 3 h (Fig. 5*E*). For the thermal test, NBI-74330 at the dose of 2 μg alleviated SNL-induced heat hyperalgesia at 1 and 3 h. The high dose (20 μg) reversed SNL-induced heat hyperalgesia (Fig. 5*F*). Furthermore, intrathecal injection of NBI-74330 (20 μg) 21 d after SNL also markedly relieved SNL-induced mechanical allodynia (Fig. 5*G*) and heat hyperalgesia (Fig. 5*H*). The same effect was observed when NBI-74330 was injected 28 d after SNL (data not shown). Collectively, the behavioral results obtained by different strategies suggest that CXCR3 play a pivotal role in the maintenance of neuropathic pain.

SNL increases CXCL10 expression in spinal neurons and astrocytes

CXCL10 is the major ligand of CXCR3 (Ransohoff et al., 2007). We examined the expression of CXCL10 in the spinal cord after SNL or sham operation. As shown in Figure 6*A*, *Cxcl10* mRNA was significantly increased at day 3, peaked at day 10, and was still elevated at day 21 in SNL mice compared with sham-operated mice. The mRNA level did not significantly differ between naive and sham-operated mice at any time point (Fig. 6*A*). ELISA results further confirmed the increased expression of CXCL10 protein in the spinal cord 10 d after SNL (Fig. 6*B*).

We then examined the expression and distribution of CXCL10 in the spinal cord by immunofluorescence staining.

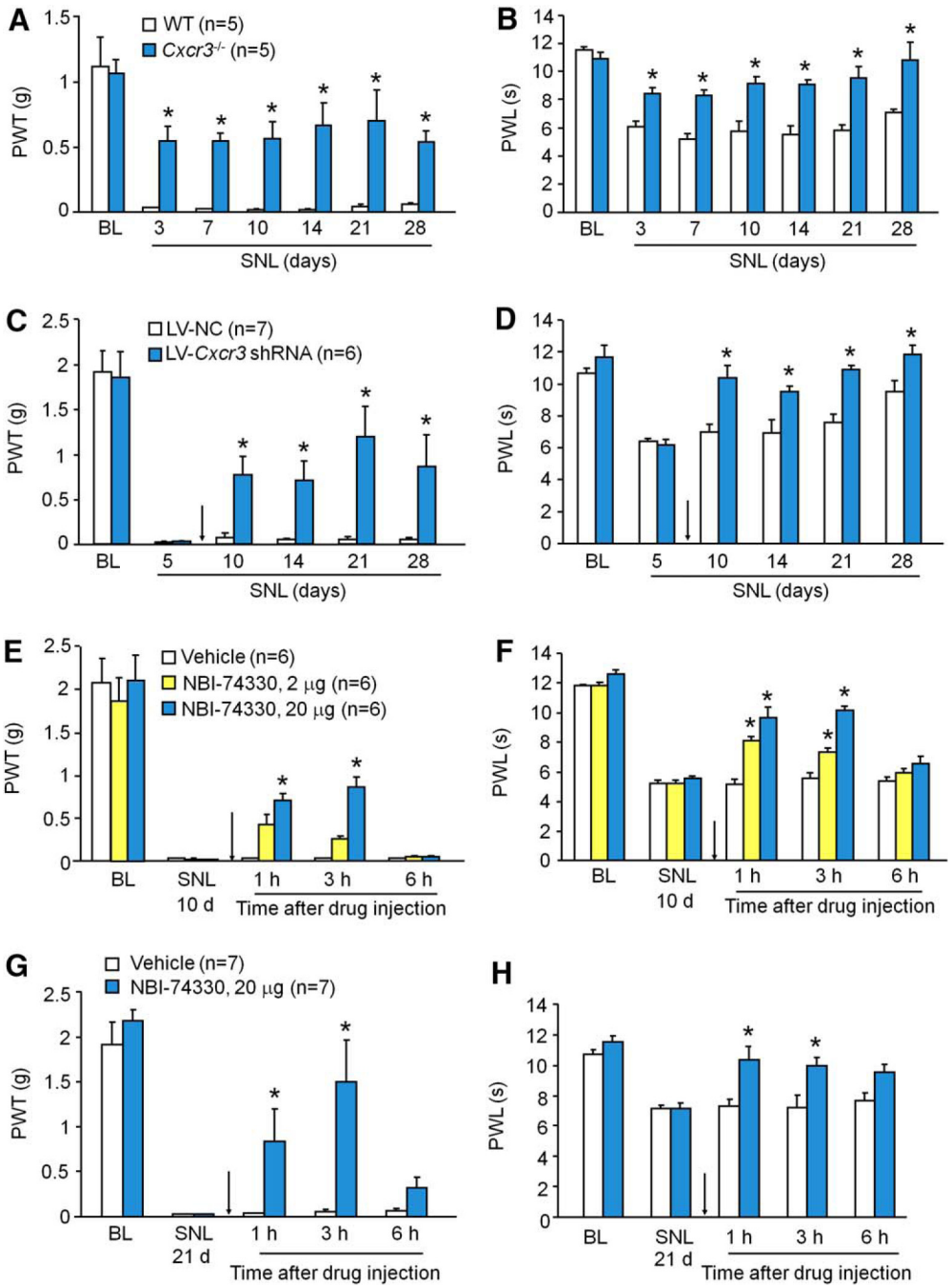

Figure 5. Deletion or inhibition of CXCR3 alleviates SNL-induced neuropathic pain. ***A***, ***B***, SNL-induced mechanical allodynia (***A***) and heat hyperalgesia (***B***) were markedly attenuated in *Cxcr3* $^{-/-}$ mice. $p < 0.05$, *Cxcr3* $^{-/-}$ versus WT. Two-way repeated-measures ANOVA followed by Bonferroni's tests. ***C***, ***D***, Intraspinal infusion of LV-*Cxcr3* shRNA lentivirus in the spinal cord 5 d after SNL persistently alleviated SNL-induced mechanical allodynia (***C***) and reversed heat hyperalgesia (***D***). *$p < 0.05$, LV-*Cxcr3* shRNA versus LV-NC. Two-way repeated-measures ANOVA followed by Bonferroni's tests. ***E***, ***F***, Intrathecal injection of CXCR3 antagonist NBI-774330 10 d after SNL transiently and dose-dependently attenuated SNL-induced mechanical allodynia (***E***) and heat hyperalgesia (***F***). ***G***, ***H***, Intrathecal injection of NBI-774330 21 d after SNL also attenuated SNL-induced mechanical allodynia (***G***) and heat hyperalgesia (***H***). *$p < 0.05$, NBI-74330 versus vehicle. Two-way repeated-measures ANOVA followed by Bonferroni's tests.

CXCL10 was expressed in the dorsal horn of naive mice (Fig. 6*C*) and sham-operated mice (Fig. 6*D*). At SNL day 10, CXCL10 immunoreactivity was markedly increased in the ipsilateral dorsal horn (Fig. 6*E*). As the cellular distribution of CXCL10 in naive and SNL mice seems different, we further did double staining. In naive mice, CXCL10 was highly colocalized with NeuN (Fig. 6*F*), sparely colocalized with GFAP (Fig. 6*G*), but not colocalized at all with CD11b (Fig. 6*H*). In SNL mice, in addition to the colocalization with NeuN (Fig. 6*I*), CXCL10 was highly colocalized with GFAP in superficial lamina (Fig. 6*J*), and not colocalized with CD11b (Fig. 6*K*). These results suggest that CXCL10 expression was constitutively expressed in spinal neurons and was increased in both neurons and astrocytes after SNL.

CXCL10 enhances excitatory synaptic transmission in spinal cord neurons via CXCR3

Since CXCR3 is mainly expressed in spinal neurons, we asked whether CXCL10 regulates neuronal function via CXCR3. We

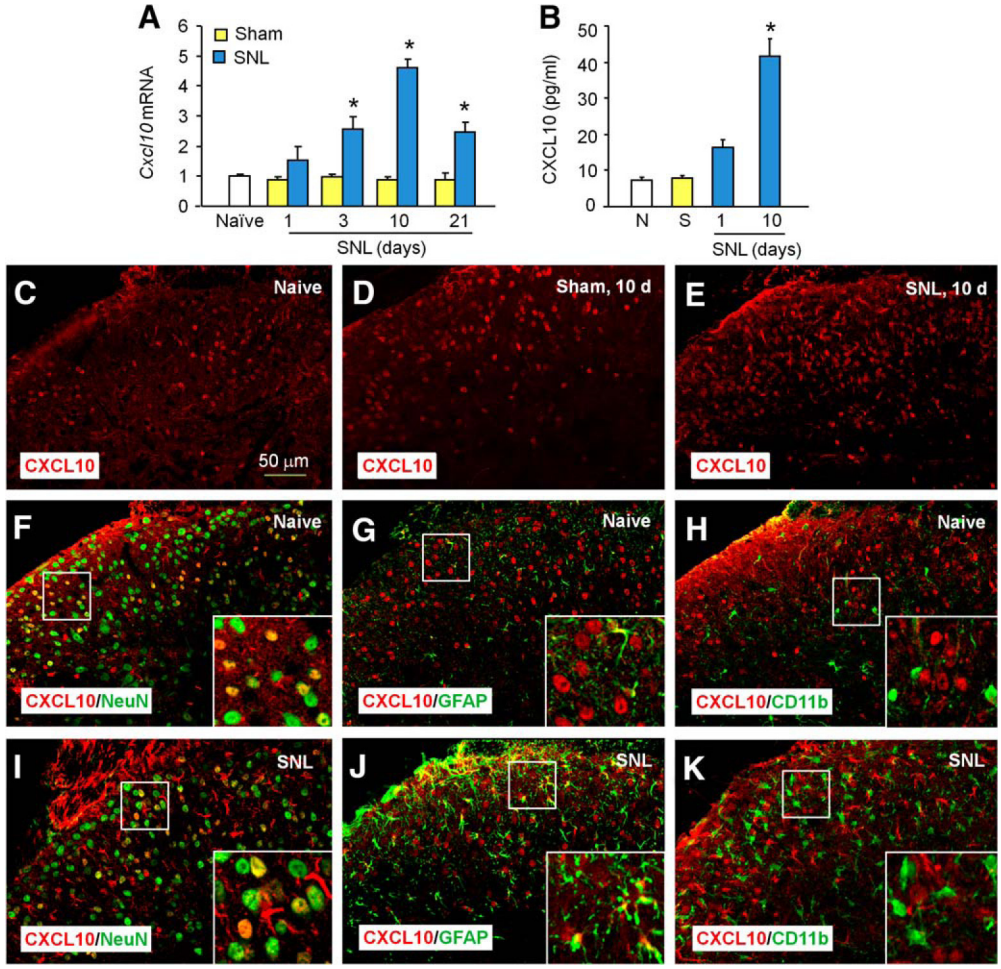

Figure 6. CXCL10 is increased in spinal neurons and astrocytes after SNL. ***A***, The time course of *Cxcl10* mRNA expression in the spinal cord from naive, sham-operated, and SNL-operated mice. SNL increased *Cxcl10* expression at 3, 10, and 21 d. *$p < 0.05$, SNL versus sham, Student's *t* test, $n = 5$ mice/group. ***B***, ELISA shows increased CXCL10 protein levels in the spinal cord 10 d after SNL. *$p < 0.05$, SNL vs sham, Student's *t* test, $n = 3$ mice/group. ***C–E***, Representative images of CXCL10 immunofluorescence in the L5 dorsal horn. CXCL10 immunoreactivity was constitutively expressed in naive mice (***C***), with similar expression in sham-operated mice (***D***) and increased expression in SNL mice (***E***). ***F–H***, Immunofluorescence double staining shows that CXCL10 was highly colocalized with NeuN (***F***), slightly colocalized with GFAP (***G***), and not at all colocalized with CD11b (***H***) in naive mice. ***I–K***, CXCL10 was colocalized with NeuN (***I***) and GFAP (***J***), but not with CD11b (***K***) 10 d after SNL.

prepared spinal cord slices and performed patch-clamp recordings in lamina II neurons in which nociceptive information is modulated and conveyed to projection neurons (Kawasaki et al., 2008). We first recorded sEPSCs from WT mice. As shown in Figure 7*A*,*B*, superfusion of CXCL10 (100 ng/ml) significantly increased the amplitude of sEPSCs in six (40.0%) neurons (1.26 ± 0.04-fold) of 15 neurons recorded from naive mice. However, the frequency was not significantly changed (1.17 ± 0.15-fold). Given that the expression of CXCR3 was increased after SNL (Fig. 1*D*), we further examined sEPSCs from mice 10 d after SNL. The same concentration of CXCL10 induced a similar increase of the amplitude of sEPSCs in 53.8% of neurons (1.22 ± 0.04-fold). In addition, the frequency of sEPSCs was increased in neurons from SNL mice (1.55 ± 0.16-fold; Fig. 7*A*,*B*). As the amplitude and frequency of the sEPSCs respectively reflects postsynaptic glutamate receptor function and presynaptic glutamate release (Kohno et al., 2005), these data suggest that CXCL10 contributes to synaptic transmission by postsynaptic mechanisms in naive mice and by both postsynaptic and presynaptic mechanisms in mice with SNL.

We then recorded sEPSCs from *Cxcr3* KO mice. Of 11 neurons recorded from mice, the sEPSC amplitude was not affected by CXCL10 (100 ng/ml) in nine. Thus, the amplitude was increased only in two (18.2%) neurons. In slices from SNL mice, none of the 11 neurons responded to CXCL10 (Fig. 7*A*). These data suggest that CXCR3 is important in CXCL10-mediated excitatory transmission of lamina II neurons.

As excitatory synaptic transmission is mainly mediated by NMDA and AMPA receptors, we further examined the effects of the CXCL10 on inward currents induced by NMDA (50 μM, 30 s) or AMPA (10 μM, 30 s) when holding the voltage at −45 and −70 mV, respectively. In WT mice, CXCL10 (100 ng/ml) significantly enhanced the inward currents elicited by NMDA in 44.4% (four of nine) neurons from naive (1.18 ± 0.03-fold) and 77.8% (seven of nine) neurons from SNL (1.33 ± 0.09-fold, Fig. 7*C*,*D*). However, in *Cxcr3* KO mice, most of the neurons were unaffected by CXCL10 (Fig. 6*C*). CXCL10 enhanced NMDA-induced currents in only 27.2% (3 of 11) neurons from naive mice and 18.2% (2 of 11) neurons from SNL mice. For AMPA-induced inward currents, CXCL10 (100 ng/ml) enhanced the currents in 33.3% (three of nine) neurons from naïve WT mice (1.25 ± 0.05-fold, $p < 0.05$) and 70.0% (7 of 10) neurons from SNL WT mice (1.33 ± 0.05-fold, Fig. 6*E*,*F*). In KO mice, CXCL10 did not change AMPA-induced currents in most of the cells (Fig. 7*E*).

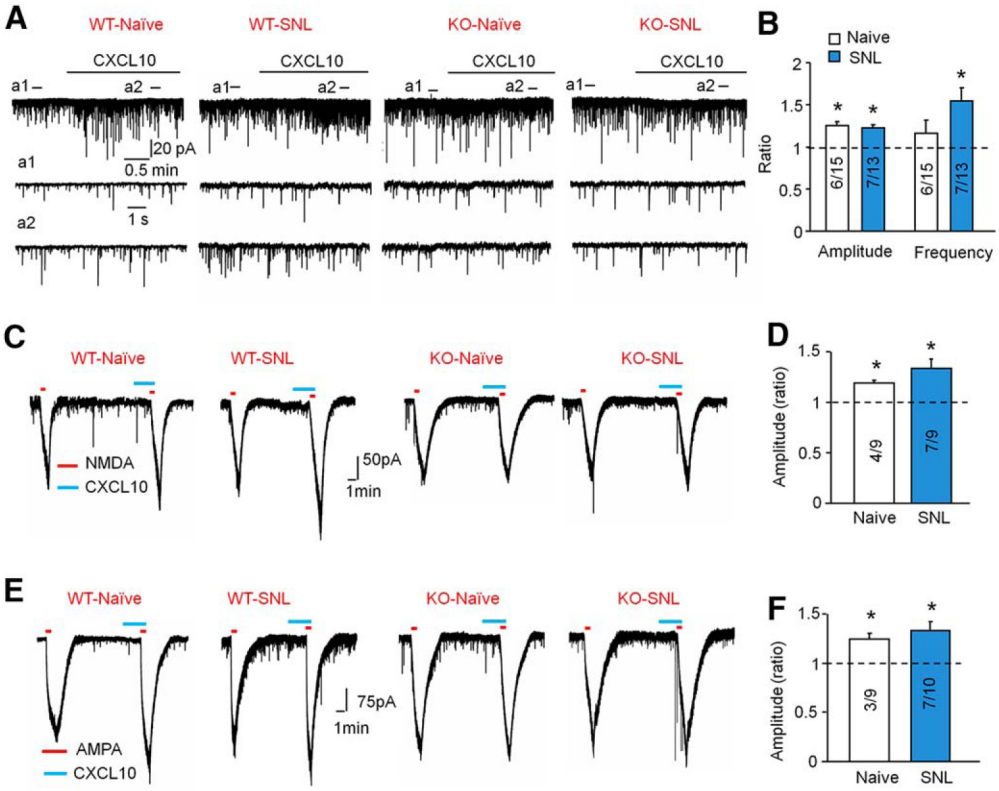

Figure 7. CXCL10 enhances excitatory synaptic transmission in lamina II neurons. ***A***, Patch-clamp recording of sEPSCs shows an increase in the amplitude of sEPSCs from WT naive animals and in both amplitude and frequency from WT SNL animals after perfusion of CXCL10 (100 ng/ml, 2 min). However, neither amplitude nor frequency was changed after perfusion of CXCL10 in slices from KO mice. a1 and a2 are enlarged recordings before and after CXCL10 treatment, respectively. ***B***, The ratio of amplitude and frequency of sEPSCs after CXCL10 treatment in WT mice. $*p < 0.05$ versus pretreatment baseline, Student's *t* test, $n = 4–5$ mice/group. ***C–F***, Patch-clamp recording demonstrates increase in NMDA-induced (***C***, ***D***) and AMPA-induced currents (***E***, ***F***) from WT mice after CXCL10 treatment (100 ng/ml). CXCL10 did not change the amplitude of NMDA-induced or AMPA-induced currents in KO mice (***C***, ***E***). The amplitude of NMDA-induced and AMPA-induced currents from WT mice is shown in ***F*** and ***H***, respectively. $*p < 0.05$ versus pretreatment baseline, Student's *t* test, $n = 4–6$ mice/group. Inside each column, the number of total recorded neurons and number of responding neurons are indicated (***B***, ***D***, ***F***).

The amplitude in only 18.2% (2 of 11) neurons from naive mice and 20% (2 of 10) from SNL mice was increased by CXCL10. These data suggest that (1) SNL increases the percentage of CXCL10-responding neurons, and (2) CXCL10 enhances NMDA-induced or AMPA-induced current via CXCR3. In addition, as CXCL10 increased sEPSCs and NMDA-induced or AMPA-induced currents in ~20% of the neurons in *Cxcr3* KO mice, researchers need to investigate whether CXCL10 has other receptors in the spinal cord.

Spinal injection of CXCL10 induces CXCR3-dependent pain hypersensitivity and ERK activation in the spinal cord

To investigate whether CXCL10 is sufficient to induce pain, we intrathecally injected CXCL10 in WT and *Cxcr3* KO mice. CXCL10, but not PBS induced mechanical allodynia in WT mice for >6 h (Fig. 8*A*), whereas CXCL10 did not significantly reduce the paw-withdrawal threshold in *Cxcr3* KO mice. Intrathecal CXCL10 also induced heat hyperalgesia in WT mice, but this hyperalgesia was abrogated in KO mice (Fig. 8*B*). These data indicate that CXCL10 is sufficient to induce pain hypersensitivity via its receptor CXCR3.

Knowing that activation (phosphorylation) of ERK in dorsal horn neurons could serve as a marker for central sensitization (Ji et al., 1999; Gao and Ji, 2009; Gao et al., 2009), we then checked pERK expression in the spinal cord after intrathecal CXCL10. CXCL10 (100 ng) induced pERK expression in the spinal dorsal horn in WT mice but not in *Cxcr3* KO mice 1 h after injection (Fig. 8*C*). Further, incubation of the spinal slices with CXCL10 (100 ng/ml, 5 min) induced a marked ERK activation in the superficial spinal cord, predominantly in the laminae I–III (Fig. 8*D*). The number of pERK-immunoreactive cells per spinal cord section increased from 5.6 ± 0.4 in control sections ($n = 8$) to 22.5 ± 2.1 in sections treated with CXCL10 ($n = 10$). Double staining showed that pERK was colocalized with NeuN (Fig. 8*E–G*), indicating that CXCL10 can activate spinal neurons.

Discussion

Accumulating evidence has shown that several chemokines and chemokine receptors are upregulated in the spinal cord in neuropathic pain (Verge et al., 2004; Zhuang et al., 2007; Gao et al., 2009; Zhang et al., 2013; Jiang et al., 2016). However, the mechanisms underlying the upregulation of these genes are not well investigated. Our study provides the first evidence that DNA demethylation of *Cxcr3* promoter in spinal neurons is involved in CXCR3 upregulation after SNL. Our results further demonstrate that *Cxcr3* demethylation, which may be caused by the downregulation of DNMT3b and decreased binding of DNMT3b with *Cxcr3*, increases the binding of transcription factor C/EBPα with *Cxcr3* and thus facilitates CXCR3 expression (Fig. 9*A*). In addition, inhibition of CXCR3 effectively attenuates neuropathic pain in mice. Finally, we found that CXCL10, a major ligand of CXCR3, is induced in spinal astrocytes and further acts on neuronal CXCR3 to enhance the excitatory synaptic transmission (Fig. 9*B*). Thus, our results reveal an epigenetic mechanism un-

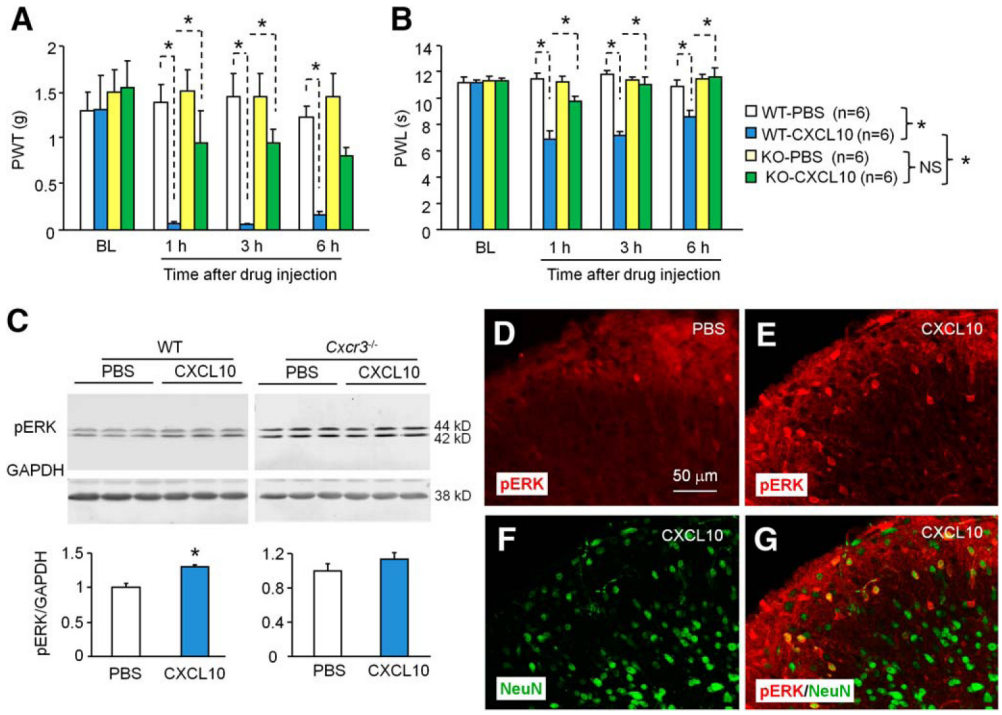

Figure 8. CXCL10 induces CXCR3-dependent pain hypersensitivity and ERK activation in spinal neurons. ***A***, ***B***, Intrathecal injection of CXCL10 (100 ng) induced mechanical allodynia (***A***) and heat hyperalgesia (***B***) in WT mice, but not in KO mice. $^*p < 0.05$, two-way repeated-measures ANOVA followed by Bonferroni's tests. ***C***, Intrathecal injection of CXCL10 increased pERK expression at 1 h in WT mice, but not in *Cxcr3* KO mice. $p < 0.05$, Student's *t* test, $n = 3$ mice/group. ***D***, ***E***, pERK expression in the spinal cord after incubation of the isolated spinal cord slices with CXCL10 (100 ng/ml, 5 min). CXCL10 induces marked ERK activation in the superficial dorsal horn. ***E–G***, Majority of pERK-immunoreactive cells were colocalized with NeuN.

derlying CXCR3 expression and the important role of CXCR3 in mediating neuropathic pain.

A growing body of evidence shows that epigenetic mechanisms, including DNA methylation, histone modification, and noncoding RNA, contribute to the regulation of gene expression (Denk and McMahon, 2012). DNA methylation is the most stable epigenetic modification, which occurs at cytosine residues, predominantly in the context of CpG dinucleotides in mammals (Jeltsch, 2002). DNA methylation is often associated with gene silencing (Kass et al., 1997). Recent studies have shown that DNA methylation is involved in chronic pain induced by nerve injury (Massart et al., 2016), inflammation (Qi et al., 2013), or diabetes (Zhang et al., 2015). We for the first time show that SNL persistently increased *Cxcr3* mRNA expression in spinal neurons, which was associated with decreased DNA methylation levels at the CpG sites within *Cxcr3* promoter region. *In vitro* experiments also confirmed that methylation of the *Cxcr3* promoter region decreased *Cxcr3* promoter activity. These data indicate that DNA methylation contributes to SNL-induced *Cxcr3* upregulation in the spinal cord.

DNA methylation can be achieved by the action of three enzymes: DNMT1, DNMT3a, and DNMT3b. DNMT1 is the key maintenance methyltransferase (Howell et al., 2001), whereas DNMT3a and DNMT3b are responsible for *de novo* methylation (Okano et al., 1999). The expression patterns of these DMNTs in the spinal cord after peripheral nerve injury, inflammation, or paw incision (Tochiki et al., 2012; Sun et al., 2015; Wang et al., 2016) are quite inconsistent, which may be due to different animal models, different species, or different time points. In the present study, neither *Dnmt1* nor *Dnmt3a* was changed, but both mRNA and protein level of DNMT3b were decreased 10 d after SNL in mice. Overexpression of DNMT3b by lentivirus increased methylation of *Cxcr3* promoter and attenuated neuropathic pain, suggesting that the methylation status of *Cxcr3* can be regulated by the expression level of DNMT3b.

C/EBPα belongs to the C/EBP family of transcription factors, which consists of six isoforms: C/EBPα, C/EBPβ, C/EBPγ, C/EBPδ, C/EBPε, and C/EBPζ (Tsukada et al., 2011). C/EBPs are widely expressed and involved in regulation of a variety of functions, including inflammation, and innate and adaptive immunity (Miller et al., 2003; Tsukada et al., 2011). C/EBPβ was recently reported to be upregulated in dorsal root ganglion neurons after SNL and may be involved in neuropathic pain via downstream signaling through TNF-α (Sasaki et al., 2014). Here our results demonstrate a pivotal role of C/EBPα in neuropathic pain via regulation of CXCR3 expression. First, the ChIP-PCR data showed that C/EBPα positively regulated *Cxcr3* transcription via direct binding to the promoter region of *Cxcr3*. Second, luciferase reporter experiments showed that binding ability of C/EBPα to *Cxcr3* promoter was enhanced when *Cxcr3* promoter was demethylated. Third, SNL increased C/EBPα mRNA and protein expression in the spinal cord, and knockdown of C/EBPα with siRNAs reduced CXCR3 expression and attenuated nerve injury-induced pain hypersensitivity. Moreover, as C/EBPα is an important transcription factor in microglia and involved in proinflammatory transcriptional activation and expression (Ponomarev et al., 2011), C/EBPα may indirectly regulate CXCR3 expression and contribute to neuropathic pain via increasing neuroinflammation (White et al., 2005; Gao and Ji, 2010).

Previous studies showed that CXCR3 was expressed in neurons of the hippocampus (Vlkolinský et al., 2004) and microglia in the entorhinal cortex (Rappert et al., 2004). In the present study, CXCR3 was found to be constitutively expressed in spinal neurons and increased after SNL. SNL also induced the expression of CXCR3 in a few microglia in the superficial dorsal horn. Moreover, CXCR3 was not only expressed in projection neurons,

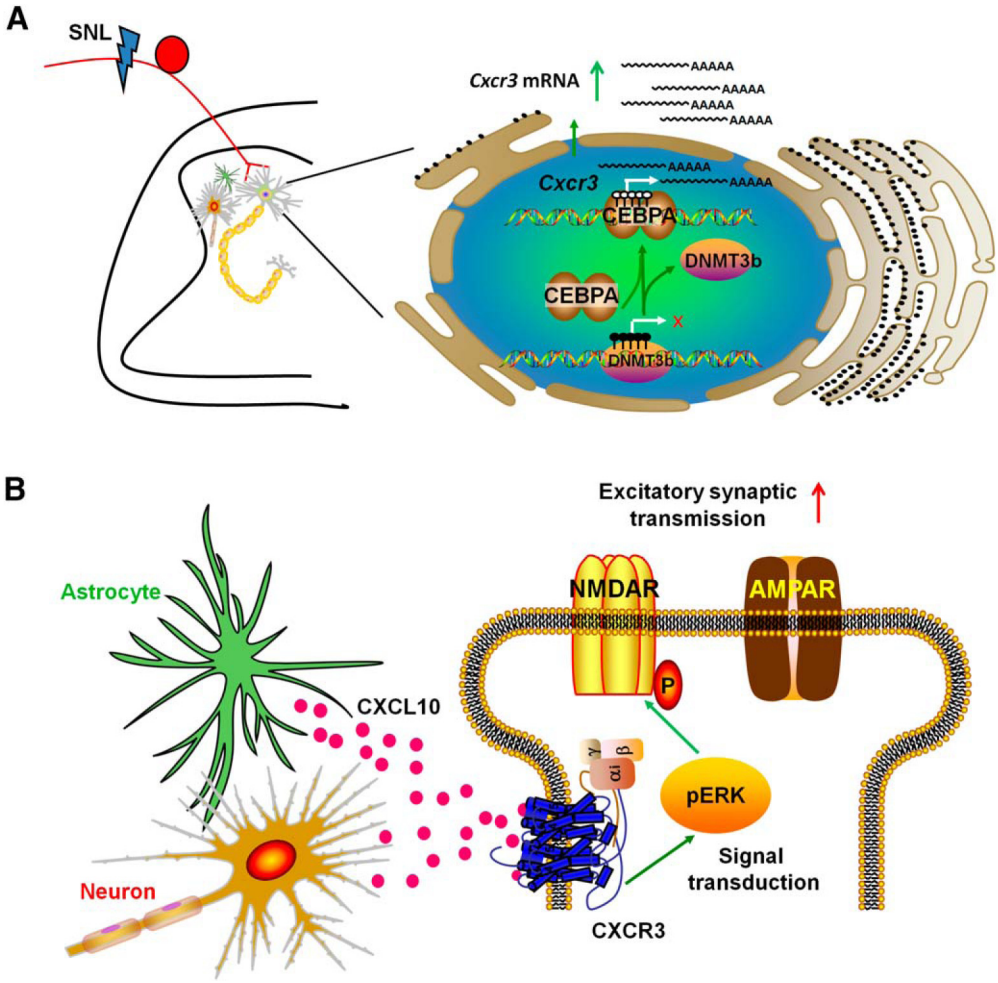

Figure 9. Schematic shows the regulation of CXCR3 expression and the involvement of CXCL10/CXCR3 in neuropathic pain. ***A***, SNL decreases the expression of DNMT3b and increased the expression of C/EBPα in the neurons of the spinal dorsal horn. The decreased DNMT3b causes DNA demethylation of *Cxcr3* promoter, which increases the binding of C/EBPα to *Cxcr3* promoter and further increases the transcription of *Cxcr3* mRNA and the expression of CXCR3 protein on cytoplasm and membrane. ***B***, SNL increases CXCL10 expression in spinal astrocytes and neurons. The released CXCL10 acts on neuronal CXCR3, which activates ERK. Activation of ERK may phosphorylate NR2B to enhance NMDA receptor activity (Hu et al., 2015) and further enhance AMPA receptor activity (Lu et al., 2001), thus increasing excitatory synaptic transmission and contributing to the pathogenesis of neuropathic pain.

also in SST$^+$-excitatory neurons and GAD2$^+$-inhibitory neurons. Recent studies have revealed that the microcircuit formed by excitatory neurons (e.g., SST$^+$ or VGLUT3$^+$) and inhibitory neurons [e.g., GAD2$^+$ or Dynorphin (Dyn)$^+$] play an important role in mechanical allodynia (Duan et al., 2014; Peirs et al., 2015). Especially, ablation of SST$^+$ neurons causes loss of mechanical pain, whereas ablation of Dyn$^+$ neurons (>80% in GAD67$^+$ neurons) induces spontaneous mechanical allodynia (Duan et al., 2014), suggesting the different role of spinal excitatory neurons and inhibitory neurons in pain modulation. Although CXCR3 is expressed in projection, excitatory, and inhibitory neurons, behavioral data showed that SNL-induced pain hypersensitivity was remarkably reduced in *Cxcr3*-deficient mice, and inhibition of CXCR3 by siRNA or antagonist alleviated established neuropathic pain, suggesting that CXCR3 in projection neurons and excitatory neurons may play a major role in mediating the maintenance of neuropathic pain. In addition, electrophysiological data (Fig. 7) showed that CXCL10 failed to increase synaptic transmission in some neurons, even after SNL. Whether these neurons are inhibitory neurons and how CXCR3 in different populations regulates pain still need to be clarified.

CXCR3 can be activated by three ligands: CXCL9, CXCL10, and CXCL11. These ligands have different temporal and spatial patterns of expression, are regulated by different stimuli, and are expressed by distinct cell types during the course of immune response (Groom and Luster, 2011; Van Raemdonck et al., 2015). As CXCL10 is a major ligand of CXCR3, and gene-expression microarray data showed that *Cxcl10* was remarkably increased after SNL (Jiang et al., 2016), we focused on CXCL10 in this study. The qPCR and ELISA data further confirmed the upregulation of CXCL10 in the spinal cord after SNL. In addition, CXCL10 was increased from 3 d after SNL, whereas SNL-induced pain hypersensitivity was shown 1 d after SNL, suggesting that CXCL10 may be induced by other mediators. Our previous study showed that CXCL10 was induced by TNF-α in cultured astrocytes (Gao et al., 2009). Consistently, immunostaining showed that CXCL10 was markedly upregulated in spinal astrocytes *in vivo*. In addition, TNF-α was rapidly (1 d) upregulated in the spinal cord after SNL (Zhang et al., 2013). Therefore, the delayed increase of CXCL10 in the spinal cord may be induced by TNF-α.

Our behavioral data showed that intrathecal injection of CXCL10 induced rapid and CXCR3-dependent pain hypersensitivity, suggesting that activation of CXCL10/CXCR3 is sufficient to induce pain. Previous studies have shown that chemokines, such as CCL2 and CXCL1, with the expression of their receptors in spinal neurons, contribute to central sensitization via in-

creased excitatory synaptic transmission (Gao et al., 2009; Zhang et al., 2013). We also found that CXCL10 increased the amplitude of sEPSCs of lamina II neurons and enhanced NMDA-induced and AMPA-induced currents via CXCR3, supporting the role of CXCL10/CXCR3 in mediating excitatory synaptic transmission. In addition, CXCL10 also increased the frequency of sEPSCs of lamina II neurons from slices after SNL, suggesting that CXCR3 in the dorsal root ganglion may also contribute to the pathogenesis of neuropathic pain.

ERK activation in dorsal horn neurons contributes importantly to the induction of central sensitization (Ji et al., 1999; Gao et al., 2009). We showed that CXCL10 induced CXCR3-dependent ERK activation in spinal neurons. As ERK is involved in the synaptic transmission mediated by GluN2B subunit-containing NMDA receptors (Hu et al., 2015), and pERK translocates to the nucleus and activates the transcription factor CREB to initiate gene transcription and maintain central sensitization and chronic pain (Ji and Strichartz, 2004), we speculate that CXCL10/CXCR3 may contribute to neuropathic pain via regulation of synaptic transmission and gene transcription.

In summary, our results for the first time demonstrate the regulation of *Cxcr3* expression in the spinal cord by DNA methylation after SNL-induced neuropathic pain. Our data support the hypothesis that the decreased expression of DNMT3b may cause the demethylation of *Cxcr3* promoter and further increase the binding of C/EBPα with *Cxcr3* to promote its transcription. Furthermore, CXCL10, expressed by spinal neurons and astrocytes, increases the excitatory synaptic transmission via CXCR3 and contributes to the maintenance of neuropathic pain. Collectively, our results suggest that targeting the expression and activation of CXCR3 may offer new therapeutics for neuropathic pain.

References

Abbadie C, Lindia JA, Cumiskey AM, Peterson LB, Mudgett JS, Bayne EK, DeMartino JA, MacIntyre DE, Forrest MJ (2003) Impaired neuropathic pain responses in mice lacking the chemokine receptor CCR2. Proc Natl Acad Sci U S A 100:7947–7952. CrossRef Medline

Abbadie C, Bhangoo S, De Koninck Y, Malcangio M, Melik-Parsadaniantz S, White FA (2009) Chemokines and pain mechanisms. Brain Res Rev 60: 125–134. CrossRef Medline

Bali P, Im HI, Kenny PJ (2011) Methylation, memory and addiction. Epigenetics 6:671–674. CrossRef Medline

Bird AP (1986) CpG-rich islands and the function of DNA methylation. Nature 321:209–213. CrossRef Medline

Denk F, McMahon SB (2012) Chronic pain: emerging evidence for the involvement of epigenetics. Neuron 73:435–444. CrossRef Medline

Descalzi G, Ikegami D, Ushijima T, Nestler EJ, Zachariou V, Narita M (2015) Epigenetic mechanisms of chronic pain. Trends Neurosci 38:237–246. CrossRef Medline

Dixon WJ (1980) Efficient analysis of experimental observations. Annu Rev Pharmacol Toxicol 20:441–462. CrossRef Medline

Duan B, Cheng L, Bourane S, Britz O, Padilla C, Garcia-Campmany L, Krashes M, Knowlton W, Velasquez T, Ren X, Ross SE, Lowell BB, Wang Y, Goulding M, Ma Q (2014) Identification of spinal circuits transmitting and gating mechanical pain. Cell 159:1417–1432. CrossRef Medline

Gao YJ, Ji RR (2009) c-Fos and pERK, which is a better marker for neuronal activation and central sensitization after noxious stimulation and tissue injury? Open Pain J 2:11–17. CrossRef Medline

Gao YJ, Ji RR (2010) Chemokines, neuronal-glial interactions, and central processing of neuropathic pain. Pharmacol Ther 126:56–68. CrossRef Medline

Gao YJ, Zhang L, Samad OA, Suter MR, Yasuhiko K, Xu ZZ, Park JY, Lind AL, Ma Q, Ji RR (2009) JNK-induced MCP-1 production in spinal cord astrocytes contributes to central sensitization and neuropathic pain. J Neurosci 29:4096–4108. CrossRef Medline

Géranton SM (2012) Targeting epigenetic mechanisms for pain relief. Curr Opin Pharmacol 12:35–41. CrossRef Medline

Groom JR, Luster AD (2011) CXCR3 ligands: redundant, collaborative and antagonistic functions. Immunol Cell Biol 89:207–215. CrossRef Medline

Hargreaves K, Dubner R, Brown F, Flores C, Joris J (1988) A new and sensitive method for measuring thermal nociception in cutaneous hyperalgesia. Pain 32:77–88. CrossRef Medline

Howell CY, Bestor TH, Ding F, Latham KE, Mertineit C, Trasler JM, Chaillet JR (2001) Genomic imprinting disrupted by a maternal effect mutation in the Dnmt1 gene. Cell 104:829–838. CrossRef Medline

Hu XD, Liu YN, Zhang ZY, Ma ZA, Suo ZW, Yang X (2015) Spinophilin-targeted protein phosphatase-1 alleviated inflammatory pain by negative control of MEK/ERK signaling in spinal cord dorsal horn of rats. J Neurosci 35:13989–14001. CrossRef Medline

Jaenisch R, Bird A (2003) Epigenetic regulation of gene expression: how the genome integrates intrinsic and environmental signals. Nat Genet 33 [Suppl]:245–254. Medline

Jeltsch A (2002) Beyond Watson and Crick: DNA methylation and molecular enzymology of DNA methyltransferases. Chembiochem 3:274–293. CrossRef Medline

Jiang BC, Cao DL, Zhang X, Zhang ZJ, He LN, Li CH, Zhang WW, Wu XB, Berta T, Ji RR, Gao YJ (2016) CXCL13 drives spinal astrocyte activation and neuropathic pain via CXCR5. J Clin Invest 126:745–761. CrossRef Medline

Ji RR, Strichartz G (2004) Cell signaling and the genesis of neuropathic pain. Sci STKE 2004:reE14. Medline

Ji RR, Baba H, Brenner GJ, Woolf CJ (1999) Nociceptive-specific activation of ERK in spinal neurons contributes to pain hypersensitivity. Nat Neurosci 2:1114–1119. CrossRef Medline

Jurkowska RZ, Jurkowski TP, Jeltsch A (2011) Structure and function of mammalian DNA methyltransferases. Chembiochem 12:206–222. CrossRef Medline

Kass SU, Pruss D, Wolffe AP (1997) How does DNA methylation repress transcription? Trends Genet 13:444–449. CrossRef Medline

Kawasaki Y, Zhang L, Cheng JK, Ji RR (2008) Cytokine mechanisms of central sensitization: distinct and overlapping role of interleukin-1beta, interleukin-6, and tumor necrosis factor-alpha in regulating synaptic and neuronal activity in the superficial spinal cord. J Neurosci 28:5189–5194. CrossRef Medline

Kohno T, Ji RR, Ito N, Allchorne AJ, Befort K, Karchewski LA, Woolf CJ (2005) Peripheral axonal injury results in reduced mu opioid receptor pre- and post-synaptic action in the spinal cord. Pain 117:77–87. CrossRef Medline

Koschmieder S, Halmos B, Levantini E, Tenen DG (2009) Dysregulation of the C/EBPalpha differentiation pathway in human cancer. J Clin Oncol 27:619–628. CrossRef Medline

Lacroix-Fralish ML, Tawfik VL, Tanga FY, Spratt KF, DeLeo JA (2006) Differential spinal cord gene expression in rodent models of radicular and neuropathic pain. Anesthesiology 104:1283–1292. CrossRef Medline

Liang L, Lutz BM, Bekker A, Tao YX (2015) Epigenetic regulation of chronic pain. Epigenomics 7:235–245. CrossRef Medline

Lindia JA, McGowan E, Jochnowitz N, Abbadie C (2005) Induction of CX3CL1 expression in astrocytes and CX3CR1 in microglia in the spinal cord of a rat model of neuropathic pain. J Pain 6:434–438. CrossRef Medline

Lu W, Man H, Ju W, Trimble WS, MacDonald JF, Wang YT (2001) Activation of synaptic NMDA receptors induces membrane insertion of new AMPA receptors and LTP in cultured hippocampal neurons. Neuron 29:243–254. CrossRef Medline

Ma X, Wang YW, Zhang MQ, Gazdar AF (2013) DNA methylation data analysis and its application to cancer research. Epigenomics 5:301–316. CrossRef Medline

Massart R, Dymov S, Millecamps M, Suderman M, Gregoire S, Koenigs K, Alvarado S, Tajerian M, Stone LS, Szyf M (2016) Overlapping signatures of chronic pain in the DNA methylation landscape of prefrontal cortex and peripheral T cells. Sci Rep 6:19615. CrossRef Medline

Miller M, Shuman JD, Sebastian T, Dauter Z, Johnson PF (2003) Structural basis for DNA recognition by the basic region leucine zipper transcription factor CCAAT/enhancer-binding protein alpha. J Biol Chem 278:15178–15184. CrossRef Medline

Okano M, Bell DW, Haber DA, Li E (1999) DNA methyltransferases Dnmt3a and Dnmt3b are essential for de novo methylation and mammalian development. Cell 99:247–257. CrossRef Medline

Peirs C, Williams SP, Zhao X, Walsh CE, Gedeon JY, Cagle NE, Goldring AC,

Hioki H, Liu Z, Marell PS, Seal RP (2015) Dorsal Horn Circuits for Persistent Mechanical Pain. Neuron 87:797–812. CrossRef Medline

Poetsch AR, Plass C (2011) Transcriptional regulation by DNA methylation. Cancer Treat Rev 37 [Suppl 1]:S8–S12. CrossRef Medline

Ponomarev ED, Veremeyko T, Barteneva N, Krichevsky AM, Weiner HL (2011) MicroRNA-124 promotes microglia quiescence and suppresses EAE by deactivating macrophages via the C/EBP-alpha-PU.1 pathway. Nat Med 17:64–70. CrossRef Medline

Qi F, Zhou Y, Xiao Y, Tao J, Gu J, Jiang X, Xu GY (2013) Promoter demethylation of cystathionine-beta-synthetase gene contributes to inflammatory pain in rats. Pain 154:34–45. CrossRef Medline

Qu L, Fu K, Yang J, Shimada SG, LaMotte RH (2015) CXCR3 chemokine receptor signaling mediates itch in experimental allergic contact dermatitis. Pain 156:1737–1746. CrossRef Medline

Ramabadran K, Bansinath M, Turndorf H, Puig MM (1989) Tail immersion test for the evaluation of a nociceptive reaction in mice. Methodological considerations. J Pharmacol Methods 21:21–31. CrossRef Medline

Ransohoff RM, Liu L, Cardona AE (2007) Chemokines and chemokine receptors: multipurpose players in neuroinflammation. Int Rev Neurobiol 82:187–204. CrossRef Medline

Rappert A, Bechmann I, Pivneva T, Mahlo J, Biber K, Nolte C, Kovac AD, Gerard C, Boddeke HW, Nitsch R, Kettenmann H (2004) CXCR3-dependent microglial recruitment is essential for dendrite loss after brain lesion. J Neurosci 24:8500–8509. CrossRef Medline

Sanchez-Mut JV, Gräff J (2015) Epigenetic alterations in Alzheimer's disease. Front Behav Neurosci 9:347. CrossRef Medline

Sasaki M, Hashimoto S, Sawa T, Amaya F (2014) Tumor necrosis factor-alpha induces expression of C/EBP-beta in primary afferent neurons following nerve injury. Neuroscience 279:1–9. CrossRef Medline

Schmitz K, Pickert G, Wijnvoord N, Häussler A, Tegeder I (2013) Dichotomy of CCL21 and CXCR3 in nerve injury-evoked and autoimmunity-evoked hyperalgesia. Brain Behav Immun 32:186–200. CrossRef Medline

Sun Y, Sahbaie P, Liang D, Li W, Shi X, Kingery P, Clark JD (2015) DNA methylation modulates nociceptive sensitization after incision. PloS One 10:e0142046. CrossRef Medline

Suzuki H, Maruyama R, Yamamoto E, Kai M (2012) DNA methylation and microRNA dysregulation in cancer. Mol Oncol 6:567–578. CrossRef Medline

Tochiki KK, Cunningham J, Hunt SP, GérantonSM (2012) The expression of spinal methyl-CpG-binding protein 2, DNA methyltransferases and histone deacetylases is modulated in persistent pain states. Mol Pain 8:14. CrossRef Medline

Todd AJ (2010) Neuronal circuitry for pain processing in the dorsal horn. Nat Rev Neurosci 11:823–836. CrossRef Medline

Toth C, Lander J, Wiebe S (2009) The prevalence and impact of chronic pain with neuropathic pain symptoms in the general population. Pain Med 10:918–929. CrossRef Medline

Tsukada J, Yoshida Y, Kominato Y, Auron PE (2011) The CCAAT/enhancer (C/EBP) family of basic-leucine zipper (bZIP) transcription factors is a multifaceted highly-regulated system for gene regulation. Cytokine 54:6–19. CrossRef Medline

Tuesta LM, Zhang Y (2014) Mechanisms of epigenetic memory and addiction. EMBO J 33:1091–1103. CrossRef Medline

Van Raemdonck K, Van den Steen PE, Liekens S, Van Damme J, Struyf S (2015) CXCR3 ligands in disease and therapy. Cytokine Growth Factor Rev 26:311–327. CrossRef Medline

Verge GM, Milligan ED, Maier SF, Watkins LR, Naeve GS, Foster AC (2004) Fractalkine (CX3CL1) and fractalkine receptor (CX3CR1) distribution in spinal cord and dorsal root ganglia under basal and neuropathic pain conditions. Eur J Neurosci 20:1150–1160. CrossRef Medline

Viet CT, Dang D, Ye Y, Ono K, Campbell RR, Schmidt BL (2014) Demethylating drugs as novel analgesics for cancer pain. Clin Cancer Res 20:4882–4893. CrossRef Medline

Vlkolinský R, Siggins GR, Campbell IL, Krucker T (2004) Acute exposure to CXC chemokine ligand 10, but not its chronic astroglial production, alters synaptic plasticity in mouse hippocampal slices. J Neuroimmunol 150:37–47. CrossRef Medline

von Hehn CA, Baron R, Woolf CJ (2012) Deconstructing the neuropathic pain phenotype to reveal neural mechanisms. Neuron 73:638–652. CrossRef Medline

Wang Y, Liu C, Guo QL, Yan JQ, Zhu XY, Huang CS, Zou WY (2011) Intrathecal 5-azacytidine inhibits global DNA methylation and methyl-CpG-binding protein 2 expression and alleviates neuropathic pain in rats following chronic constriction injury. Brain Res 1418:64–69. CrossRef Medline

Wang Y, Lin ZP, Zheng HZ, Zhang S, Zhang ZL, Chen Y, You YS, Yang MH (2016) Abnormal DNA methylation in the lumbar spinal cord following chronic constriction injury in rats. Neurosci Lett 610:1–5. CrossRef Medline

White FA, Wilson NM (2008) Chemokines as pain mediators and modulators. Curr Opin Anaesthesiol 21:580–585. CrossRef Medline

White FA, Bhangoo SK, Miller RJ (2005) Chemokines: integrators of pain and inflammation. Nat Rev Drug Discov 4:834–844. CrossRef Medline

Zeilhofer HU, Wildner H, Yévenes GE (2012) Fast synaptic inhibition in spinal sensory processing and pain control. Physiol Rev 92:193–235. CrossRef Medline

Zhang HH, Hu J, Zhou YL, Qin X, Song ZY, Yang PP, Hu S, Jiang X, Xu GY (2015) Promoted interaction of nuclear factor-kappaB with demethylated purinergic P2X3 receptor gene contributes to neuropathic pain in rats with diabetes. Diabetes 64:4272–4284. CrossRef Medline

Zhang ZJ, Cao DL, Zhang X, Ji RR, Gao YJ (2013) Chemokine contribution to neuropathic pain: respective induction of CXCL1 and CXCR2 in spinal cord astrocytes and neurons. Pain 154:2185–2197. CrossRef Medline

Zhuang ZY, Kawasaki Y, Tan PH, Wen YR, Huang J, Ji RR (2007) Role of the CX3CR1/p38 MAPK pathway in spinal microglia for the development of neuropathic pain following nerve injury-induced cleavage of fractalkine. Brain Behav Immun 21:642–651. CrossRef Medline

Zovkic IB, Guzman-Karlsson MC, Sweatt JD (2013) Epigenetic regulation of memory formation and maintenance. Learn Mem 20:61–74. CrossRef Medline